THE EFFECT OF LIGHT EMITTING DIODE (LED) ON THE HEALING OF ENDOSSEOUS INTRAORAL IMPLANTS

By

Mahdi Ghuloom

A thesis submitted in conformity with the requirements

for the degree of Master of Science

Graduate Department of Dentistry

University of Toronto

THE EFFECT OF LIGHT EMITTING DIODE (LED) ON THE HEALING OF ENDOSSEOUS INTRAORAL IMPLANTS

Mahdi Ghuloom 2012, Degree of Master of Science, Graduate Department of Dentistry, University of Toronto

Abstract

Background: Implant stability may be affected by initial resorption of bone at the implant surface. This may dictate the timing of implant loading. Since the discovery of osseointegration, scientists and clinicians have been investigating methods to enhance osseointegration by improving implant characteristics and enhancing the environment around the dental implant to provide optimal conditions for bone integration. Several *in vivo* and *in vitro* studies have demonstrated that the use of photobiomodulation may improve bone repair in surgical defects. Greater and faster bone formation was seen in irradiated defects and surgical wounds when compared with control groups.

Objective: 1) To assess the role of photobiomodulation on the early bone tissue healing period applied to the practice of endosseous dental implants using a randomized clinical trial (RCT). 2) To assess the role of photobiomodulation on peri-implant alveolar crestal bone in the early healing period of bone tissue.

Materials and Methods: After obtaining REB from the University of Toronto, a total of 72 patients requiring 76 dental implants (35 female and 37 male; mean age 63.5; range 35-100 years) were recruited and consented for inclusion into

this trial. Patients received dental implants by a single operator. Implants were randomly assigned to one of two groups, control (n=47), and treatment group (n=29). All patients in the study received dental implant(s.) The treatment group had to apply light emitting diode (LED) delivered by OsseoPulse device to the surgical site, while the control group did not. Patients in the treatment group were educated on how to use the OsseoPulse device and were instructed to apply it to the surgical site preoperatively for 20 minutes, and for additional 10 daily sessions of 20 minutes each postoperatively starting the day of surgery. Implant stability was assessed using the Osstell device which utilizes resonance frequency analysis (RFA) technology and expresses data as Implant Stability Quotient (ISQ) values. ISQ of the implants was measured at time of surgery immediately following implant placement. It was also reassessed on a frequent basis in weeks 1, 2, 4, and 8 post operatively. The radiographs were taken immediately after insertion and at 8 weeks follow-up appointment. Radiographs were analyzed using SigmaScan Pro and the data were analyzed statistically using SPSS and Stata.

Results: As expected, there was a continuous decrease in ISQ value in the control group over the first 4 weeks following implant placement. This was followed by an increase at 8 weeks post-operatively. On the other hand, this ISQ decrease was not seen in the treatment group; instead, there was a continuous increase in ISQ values over the follow-up period. A significant change in ISQ values ($p < 0.001$) was seen between the groups at every follow-up visit in comparison to initial visit. Regression analysis study showed that the primary

effect of LED on ISQ values was seen over the first 2 weeks ($p < 0.05$). The mean crestal bone loss among the control was significantly greater than the treatment group at 8 weeks ($p = 0.05$).

Conclusions: Data suggest that photobiomodulation by means of LED will allow for a continuous increase in ISQ value and may reduce crestal bone resorption in the early phases of bone healing around dental implants.

I dedicate this thesis to my parents and my beloved children,

Yousif and Zahraa

Acknowledgement

I would like to acknowledge those who have supported me throughout this thesis. I would like to thank my advisory committee members and mentors, Dr. Cameron Clokie, Dr. Gerald Baker, Dr George Sándor, and Dr. Howard Holmes for their dedication, mentorship, careful revisions, and guidance over the last four years.

Thanks to Kevin Strange, Dr. Peter Brawn, Dennis Ma, and Ryan Bredin from Biolux Research Ltd. for providing me with their unlimited support to undertake this project.
I would also like to thank Osstell AB, represented by Ola Olsson, for their generosity in supporting this project.

I wish to thank Dr. Ira Schecter for his extraordinary dedication in treating the patients and collecting the data in this trial.

I would like to acknowledge Dr. Sean Peel, Nancy Valiquette, Aileen Zhou, and Dr. Ashkan Ebrahimpour for their endless support and technical advices.

Many thanks to Dr. Dena Taylor for her honest and thorough editorial advice.

I would like to thank my co-residents, Joel Abikhzer and Christa Favot for their friendship, support and encouragement over the years. They made this residency tolerable.

A special thank you to Golnaz for her never-ending inspiration and support throughout this endeavor.

In addition, I would like to express my gratitude to my family for their love, support, and prayers. Despite the distance, they were always there for me.

Lastly, I would like to thank my beautiful children, Yousif and Zahraa. I might have been far from them, but their love kept me going.

Table of Contents

ABSTRACT.....**ii**

ACKNOWLEDGEMENT.....**vi**

LIST OF TABLES .....**xii**

LIST OF FIGURES.....**xiii**

ABBREVIATIONS .....**xiv**

SYMBOLS.....**xviii**

CHAPTER I: THESIS INTRODUCTION **1**

1.1 INTRODUCTION.....**2**

1.2 PERI-IMPLANT OSSEOUS HEALING.....**3**

1.3 IMPLANT LOADING.....**6**

1.4 IMPLANT STABILITY **7**

1.5 PHOTOBIOMODULATION (PBM).....**13**

1.5.1 Introduction.....13

1.5.2 Lasers 15

1.5.3 Low Level Laser 16

1.5.4 Light emitting diode (LED) 17

1.5.5 LED versus LLLT as a source of photobiomodulation.....19

1.5.6 The physics of light-tissue interaction 22

1.5.7 Mitochondrial ATP production.....23

1.5.8 Photobiomodulation mechanism of action (MOA) 27

1.6 APPLICATIONS OF PHOTOBIOMODULATION.....**37**

1.6.1 Role of photobiomodulation in wound healing....37
1.6.2 Role of photobiomodulation in neural protection....38
1.6.3 Role of photobiomodulation in nerve regeneration....38
1.6.4 Role of photobiomodulation in pain modulation....39
1.6.5 Role of photobiomodulation bone regeneration and implant healing....40
1.7 TREATMENT DOSE....42
1.7.1 Biphasic dose response (BDR)....43
1.8 LIMITATIONS OF STUDIES IN THE FIELD OF PHOTOBIOMODULATION....44
1.9 GOAL OF STUDY....45
CHAPTER 2: OBJECTIVE AND HYPOTHESIS....46
2.1 OBJECTIVE....47
2.2. HYPOTHESIS....47
CHAPTER 3: MATERIALS AND METHODS....48
3.1 STUDY POPULATION....49
3.2 INTRAORAL IMPLANT THERAPY....50
3.3 LED TREATMENT PROTOCOL....51
3.4 FOLLOW-UP PROTOCOL....54
3.5 DATA COLLECTION....54
3.6 STATISTICAL ANALYSIS....60
CHAPTER 4: RESULTS....61
4.1 INTRODUCTION....62

4.2 INDEPENDENT VARIABLES 64

4.2.1 AGE.....64

4.2.2 GENDER 65

4.2.3 IMPLANT LOCATION IN THE MOUTH 66

4.2.4 RIDGE TYPE 67

4.2.5 BONE QUALITY 68

4.2.6 IMPLANT DIAMETER.....69

4.2.7 IMPLANT LENGTH.....70

4.2.8 IMPLANT SURFACE 71

4.3. ISQ AVERAGES OVER FOLLOW-UP PERIOD 72

4.4. ISQ CHANGE FROM INITIAL MEASUREMENT.....74

4.5. ISQ PERCENTILE CHANGE FROM INITIAL MEASUREMENT.....77

4.6. ISQ CHANGE FROM PREVIOUS MEASUREMENT.....80

4.7 REGRESSION ANALYSIS OF THE INDEPENDENT VARIABLES AT POINT ZERO82

4.8 TIMING THE EFFECT OF PHOTOBIOMODULATION DURING THE OF PERI-IMPLANT HEALING PERIOD 84

4.9 RADIOGRAPHIC ANALYSIS OF CRESTAL BONE LOSS 86

CHAPTER 5: DISCUSSION 87

5.1 INTRODUCTION.....88

5.2 INDEPENDENT VARIABLES AT POINT ZERO 88

5.3 IMPLANT STABILITY AT POINT ZERO.....89

5.4 IMPLANT STABILITY CHANGE OVER 8 WEEKS 92

5.5 THE EFFECT OF PHOTOBIOMODULATION 94

5.6 PHOTOBIOMODULATION EFFECT ON CRESTAL BONE LOSS 95

5.7 STUDY LIMITATIONS 96

5.8 FUTURE DIRECTIONS 98

CHAPTER 6: CONCLUSION 99

REFERENCES 97

List of Tables

Table 3.1. Parameters of LED that were used in this study……53

Table 4.1. Age comparison ……..65

Table 4.2. Gender comparison ……...66

Table 4.3. Implant location comparison ……..…67

Table 4.4. Ridge type comparison…….……....68

Table 4.5. Bone quality at site of implant comparison ……....69

Table 4.6. Implant diameter (as groups) comparison……70

Table 4.7. Implant length (as groups) ……..……71

Table 4.8. Implant surface area (as groups)……72

Table 4.9. Statistical analysis of mean total ISQ change from initial measurement…….....77

Table 4.10. Statistical analysis of mean ISQ percentile (%) change from initial measurement……...80

Table 4.11. Statistical analysis of mean ISQ change from previous measurement……..83

Table 4.12. Regression analysis of independent variables affecting ISQ at point zero……..…….…84

Table 4.13. Timing the effect of photobiomodulation ……..……86

Table 4.14. Crestal bone percentile changes at 8 weeks…….……....87

List of Figures

Figure 1.1. The Osstell device……...11-12

Figure 3.1. The OsseoPulse device……...54

Figure 3.2. Data collection sheet…….…….57-58

Figure 3.3. Measuring crestal bone height medially and distally in relation to implant length immediately after implant insertion……..59

Figure 3.4. Measuring crestal bone height medially and distally in relation to implant length at 8 weeks after implant insertion…….60

Figure 4.1. ISQ averages over follow-up period (8 weeks)……..……...…73

Figure 4.2. Mean total ISQ change from initial measurement……75

Figure 4.3. Mean ISQ percentile change from initial measurement……..78

Figure 4.4. Mean change of ISQ from previous measurement……...……81

Abbreviations

Acetyl-CoA	Acetyl coenzyme A
ADP	Adenosine diphosphate
ATP	Adenosine triphosphate
Avg	Average
BDR	Biphasic dose response
BG	Band gap
Ca^{2+}	Calcium
$[Ca^{2+}]$	Concentration of Ca^{2+}
cAMP	Cyclic adenosine monophosphate
CB	Conduction band
CCO	Cytochrome c oxidase
DNA	Deoxyribonucleic acid
EC	Electrochemical
EMS	Electromagnetic spectrum
ETC	Electron transport chain
F	Female
GFs	Growth factors
GSR	Glutathione reductase
GSH	Glutathione
GSSG	Glutathione disulfide couple
H^+	Hydrogen ions
HIF-1	Hypoxia-inducible factor-1

H_2O	Water
H_2O_2	Hydrogen peroxide
IκBs	Inhibitors of NF-κB
IKK	IκB kinase
IL-1β	Interleukin1-beta
ISQ	Implant Stability Quotient
J/cm²	Joules per centimeter squared
KCN	potassium cyanide
LED	Light emitting diode
LLL	Low level laser
LLLT	Low level laser therapy
LPS	Bacterial lipopolysaccharides
M	Male
MOA	Mechanism of action
mRNA	Messenger ribonucleic acid
mW	Milliwatts
MWU	Mann-Whitney U test
NAD	Nicotinamide adenine dinucleotide
NADP	Nicotinamide adenine dinucleotide phosphate
NAP	Neutrophil activating peptides
Ncm	Newton centimeter
NF-kB	Nuclear factor kappa-light-chain-enhancer of activated B cells
NGF	Nerve growth factor

NIR	Near-infrared
nm	Nanometer
NO•	Nitric oxide
NT	Neurotransmitters
O_2	Molecular oxygen
$O_2^{-\bullet}$	Superoxide anion
OH•	Hydroxyl radical
OPG	Osteoprotegerin
PBM	Photobiomodulation
PDGF	Platelet-derived growth factor
PDT	Photodynamic therapy
RANK	Receptor activator nuclear factor kappa B ligand
RANKL	RANK ligand
RCT	Randomized clinical trial
RFA	Resonance frequency analysis
ROS	Reactive oxygen species
RNS	Reactive nitrogen species
SERCA	Sarcoplasmic reticulum Ca^{2+} ATPase
SOD	Superoxide dismutases
SR	Sarcoplasmic reticulum
StD	Standard deviation
TF	Transcription factors
TGF-β	Transforming growth factor beta

TMD	Temporomandibular disorders
TNFα	Tumor necrosis factor alpha
TR	Thioredoxin reductase
$Trx(SH)_2$	Thioredoxin
TrxSS	Thioredoxin disulfide couple
VB	Valence band
VEGF	Vascular endothelial growth factors
W	Watts

Symbols

λ Wavelength

Chapter I: Thesis

Introduction

1.1 Introduction

Humans have been faced with the problem of tooth loss since the beginning of the time. As a result, we have been on a constant mission to find options to restore lost teeth (1). However, most attempts were unsuccessful or unpredictable until the innovative discovery of endosseous intraoral dental implants by Professor Brånemark (2). Brånemark used implants made of titanium, and they were integrated in bone tissues via what was described as the process of “osseointegration”. Osseointegration is the phenomenon of direct contact of living bone with a biocompatible implant in the absence of an interposing soft tissue layer at the resolution of the light microscope (3, 4).

The discovery of osseointegration has in turn led to a continuous effort to enhance and speed the process. Ongoing extensive *in vivo* and *in vitro* research supplemented with clinical trials has been conducted in order to reach these objectives (5-8).

In general, methods to enhance osseointegration can be categorized in two ways. First are those that attempt to improve implant characteristics such as implant biomaterials, implant design, surface topography, surface energy, and surface chemistry (5-8). The second category includes enhancing the environment around the dental implant to provide an optimal medium for its osseointegration in biological tissues. Researchers and clinicians, for example, have incorporated cytokines, growth factors, gene therapy,

and photobiomodulation using a low level laser therapy (LLLT) or light emitting diode (LED) (9-16).

1.2 Peri-implant osseous healing

Upon injury, the biologic response is to faster healing through a reparative or a regenerative process depending on the tissue type and condition. Aside from bone and embryonic tissues, the reparative response of all other tissues leads to fibrous connective tissue scar formation that does not resemble the original tissue in structure and function (1, 17). On the other hand, bone is capable of regeneration under favorable conditions. Regeneration results in tissues that have the same structure and function as the original tissue prior to injury (1, 17).

The preparation of a surgical site and then placement of an endosseous dental implant is an example of iatrogenic tissue injury. Endosseous implants are osseointegrated via bone regeneration around the implant (17). However, if the conditions are not optimal, bone heals in a reparative fashion leading to a fibrous integration of the implant (1).

In general, biological wounds heal in three phases that overlap, but are physiologically distinct: inflammatory, proliferative, and maturation phases. Bone fracture healing follows this pattern. Endosseous implant healing, which resembles in many aspects the

healing of bone fracture, follows this pattern as well, even though different terminology is used to describe the peri-implant bone healing phases (1, 17).

Implant site preparation in bone results in intra-osseous hemorrhage that leads to clot formation around the implant immediately after placement. Achieving a perfect implant-bone fit is not possible due to gaps between the implant surface and the edge of the endosseous osteotomy. These gaps fill with blood forming a blood clot, or hematoma, which persists for a few days. The blood clot is primarily composed of platelets (17, 18), which then become activated (19-22). The activation is enhanced by the implant's surface micro-topography. Upon activation, platelets release growth factor and cytokines, such as platelet-derived growth factor (PDGF), transforming growth factor beta (TGF-β), vascular endothelial growth factors (VEGF), and neutrophil activating peptides (NAP). The released cytokines and growth factors are crucial in multiple processes in the early phases of implant healing: they are responsible for chemoattracting and activating neutrophils involved in the inflammatory phase of wound healing. They chemoattract mesenchymal cells. They stimulate osteoinduction, which is the process of converting osteogenic mesenchymal cells into bone matrix producing mature osteoblasts. They also facilitate the process of osteoconduction (bone growing on implant or bone surfaces). They then stimulate new vascular formation (angiogenesis) in order to maintain cell vitality, which leads to the formation of new bone (19-21, 23).

Platelets are also responsible for triggering the coagulation cascade and ultimately fibrin network formation. A fibrin network attaches to the implant surface. Osteoblasts migrate through this network to the implant surface prior to producing bone matrix on the implant surface (19-22). Within the osteotomy itself, disruption of blood vessels is seen, as well as early inflammatory changes resulting in tissue hypoxia and a decrease in tissue pH. These changes also stimulate angiogenesis.

Following the aforementioned early events, bone healing around implants can be subdivided into three phases: osteoconduction, *de novo* bone formation, and bone remodeling (19-21).

Bone grows by apposition or layering. Once mesenchymal cells are induced into becoming osteoblasts, they attach themselves onto the bone surface and start secreting extracellular bone matrix to be calcified later. Bone continues to grow inward toward the implant. This process is called distant osteogenesis. On the other hand, differentiated osteoblasts adjacent to the implant surface attach themselves onto the implant surface and start secreting extracellular bone matrix in a layering fashion onto the surface. This process of new bone formation on the surface of the implant is termed *de novo* bone formation. Contact osteogensesis is the term given to the processes of osteoconduction and *de novo* bone formation when they occur together on the surface of the implant during the early phases of healing. This process occurs rapidly, and is predominantly seen with cancellous bone (19-22). In class IV bone (24) this process is required in order to obtain stability of implant.

Bone remodeling is a slow and ongoing process that occurs in response to implant loading. It occurs as a function of osteoclasts' and osteoblasts' continuous activity in order to replace the immature woven bone that is deposited early into a more mature lamellar bone. This process is the predominant event that occurs during the cortical bone healing around implants (19-21). It also occurs in order to maintain bone homeostasis as the body continues to replace its volume at a rate of 0.5% of its volume daily via this process (25).

1.3 Implant loading

Implant dentistry is an evolving science. Since the early studies of Dr. Brånemark in the 1960s and 1970s, an ongoing effort has been made to reduce the time of osseointegration and ultimately to reduce the time it takes to load the implant (26).

Early clinical protocols utilized a two-stage surgical approach in order to obtain reproducible and successful outcomes. This involved submerging the implant under the submucosal tissue after implantation into bone. In a secondary surgery, the implant was exposed trans-orally prior to loading with the prosthetic components (4). Later studies demonstrated that a single-stage surgery technique was an acceptable alternative. During this procedure, a healing abutment that is exposed trans-orally is attached to the implant, eliminating the need for a secondary surgery (27-29). These early protocols emphasized a waiting period of three to eight months of healing prior to loading the

implant with prosthetic components following a two-stage surgical approach. However, clinical research has shown that in select circumstances, the option of earlier loading of implants may be considered an acceptable option. The healing period following single-stage surgical approach, prior to loading of implants, has been shortened to 6-8 weeks (6, 30). Recent clinical studies have introduced the concept of immediate loading in order to achieve an increase in patient satisfaction and patient acceptance rate for implants. Immediate loading is defined clinically as loading the implant with prosthetic components within 48-72 hours after insertion into bone (31).

Studies have shown that immediate loading of dental implants is a valid option as long as certain prerequisites are met. The most important of these are adequate primary stability upon insertion and minimal loading of the implants, which will reduce mechanical stress and minimize micro-movement in order to allow for successful osseointegration (26, 32).

1.4 Implant stability

The stability of an implant in bone is a necessity for successful osseointegration and hence loading of the implant with a dental prosthesis. Stability is divided into categories: primary and secondary (33). Primary is the stability of the implant obtained at the time of insertion into bone. It is obtained by the biomechanical interlocking of the implant and bone tissue. It is dependent primarily upon bone quality, quantity, implant design, and

surgical technique (22, 31, 34). However, the areas of bone contacting the implant surface are subsequently slowly resorbed by osteoclastic activity. This decreases the initial primary mechanical stability of the implant. Secondary stability is a biological event. It is achieved by the early deposition of new bone around the implant surface, as discussed above, and commences within a few days of implantation. Both the primary and secondary stability are crucial for successful osseointegration. At any given point of time during the early phases of implant healing, total stability can be viewed as a combination of the two stability processes. As the initial stability of an implant decreases, secondary stability increases until the completion of the healing process. Nevertheless, there is a period when implant stability is compromised because the rate of decrease in primary stability is faster than achieving adequate secondary stability. The implant is at a higher risk of failure during this period if optimal conditions are not ensured, such as lack of micro-motion (33, 35). This critical period has been estimated to be 2 to 3 weeks following implant placement, and has been extrapolated from histological animal studies using dog model (33, 35).

Attempting to develop a protocol to reduce the loading time of implants requires a valid and reliable method to quantify the stability of implant in bone tissue. This is important to assess primary stability. In order to quantify stability of implants, multiple methods have been used in the past such as insertion torque, Periotest, and resonance frequency analysis (RFA).

Studies have demonstrated that using insertion torques of 32 to 45 Newton centimeters (Ncm), as recorded by a manual torque wrench or motor hand-piece, is an adequate indicator of primary stability (36-38).

Periotest (Medizintechnik Gulden, Germany) is an electromechanical device that, upon tapping the implant with a small integrated hammer at a specified speed, measures the deceleration of the hammer. This change in speed is processed electronically and the outcome value is correlated to implant stability (39).

The most commonly used RFA-based device in implant dentistry is the Osstell ISQ (Osstell AB, Göteborg, Sweden). A wireless SmartPeg is attached to the implant. Osstell provides a wide selection of SmartPegs that can fit on the majority of different implant systems and are adaptable to different implant diameters (Figure 1.1 a,b). The technique is non-invasive. The Osstell device, wirelessly and without contacting the SmartPegs, creates a variable frequency magnetic pulse that vibrates the SmartPeg (Figure 1.1 c). In turn, the vibration of the SmartPeg causes the implant embedded in bone to vibrate in a resonance frequency that the Osstell device can measure. The vibrations induce a lateral bending force on the implant that resembles clinical loading conditions but at a lower magnitude (Figure 1.1 d). The Osstell converts the resonance frequency into arbitrary values ranging from 1 to 100 (Figure 1.1 e). This value is designated as the Implant Stability Quotient (ISQ). The higher the ISQ value, the more rigid the implant-bone interface is, and hence the increased stability of the implant.

Studies have suggested that implants with ISQ values above 54 are considered to be stable and are amenable to immediate loading (40-45).

In our study, the Osstell ISQ device was used to assess the effect of photobiomodulation on the early bone healing around dental implants.

(a)

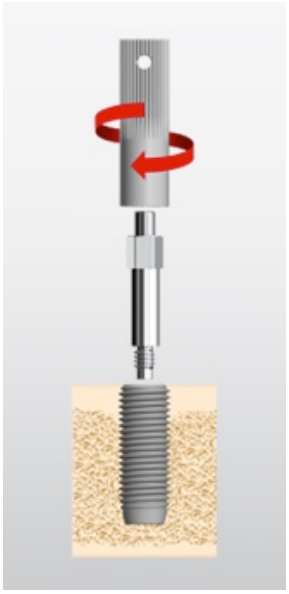

(b)

(c)

Figure 1.1: Osstell device: parts and clinical application: (a) SmartPeg; (b) SmartPeg is attached to the implant after implant insertion; (c) Osstell device creates a variable frequency magnetic pulse that vibrates the SmartPeg.

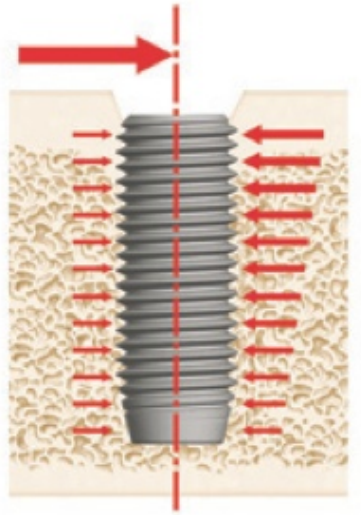

(e)

(d)

Figure 1.1 (continued): Osstell device: parts and clinical application: (d) Pulse from Osstell device induces lateral bending force on the implant that resemble clinical loading condition; (e) Osstell device showing the ISQ value on its monitor. (Images are reprinted with permission from Osstell: www.osstell.com)

1.5 Photobiomodulation (PBM)

1.5.1 Introduction

Light is a form of electromagnetic energy that exists as particulate matter and travels in waves having a constant velocity. The basic unit of light is called a photon. Light energy is composed of photons or discrete packets of electromagnetic energy. Waves of photons have different amplitudes and different wavelengths. Amplitude is defined as the absolute value of the maximum vertical displacement from a zero value during one period of an oscillation, while wavelength (λ) is defined as the distance between one peak or crest of a wave of light, heat, or other energy and the next corresponding peak or crest. Amplitude correlates with the intensity or brightness of light and is measured in joules (J), which is the unit of energy. Wavelength is measured in nanometers (nm). Nanometer is a metric unit of length and is equivalent to one billionth of a meter. Wavelength may affect how light is delivered to a target, and thereby, how light can react with tissues. It is important to appreciate that the energy of an individual photon depends on its wavelength (46, 47).

Light therapy has been used in many cultures for thousands of years as a therapeutic modality to treat various health conditions (48). Sunlight was used as the earliest form of light therapy. However, over the past two centuries alternative methods of delivering light were developed and light, as a treatment modality, evolved for two primary

reasons. The first was the extensive work of Niels Ryberg Finsen, a nineteenth-century Danish physician who realized that the refractive rays from the sun, or as he called them, the “chemical rays,” may have a stimulating effect on biological tissues. He demonstrated that by using an artificial light source to concentrate the “chemical rays,” beneficial effects were seen in the treatment of *lupus vulgaris*, a disfiguring skin disease. He was awarded The Nobel Prize in 1903 for his work (49, 50). The second was the discovery of lasers in the 1960s (51).

Bio-photonics is defined as the science of generating and harnessing light (photons) to image, detect, and manipulate biological materials. It integrates lasers, nanotechnology, and biotechnology. It is applied in medicine and dentistry as an aid in the fields of diagnostics, therapeutics, and research (52).

Medical therapeutic effects of light include but are not limited to thermal interaction, photodynamic therapy, and photobiomodulation. Thermal interaction occurs when heat is generated by high energy light and this can be used to disrupt tissues. This approach can mechanically induce ablation, coagulation, vaporization, carbonation, and melting. This application is used to control surgical bleeding or to incise tissues. Photodynamic therapy involves the application of a photosensitizing agent (porphyrin based, chlorophyll based, or a dye) which will interact with light to trigger chemical reactions in the body. Photobiomodulation may be induced using low level lasers (LLL) or light emitting diodes (LED) that stimulate photochemical effects on tissues without producing

heat which could damage biological tissues (52). The therapeutic effect of LLL therapy (LLLT) and LED to induce photobiomodulation was our primary focus in this study.

Endre Mester, a Hungarian physician, conducted multiple laser experiments in the 1960s to assess their carcinogenic potential. Using low energy ruby red laser with mice, he demonstrated improved hair growth instead of causing cancer. This was the first demonstration of “photo-biostimulation” (47, 48, 53). Subsequently, these results led to further studies assessing the influence of red light on wound healing. The term photobiomodulation was introduced later and it was demonstrated that the effects of radiation could be either stimulatory or inhibitory (54, 55). Photobiomodulation is applied in many areas of medicine such as wound healing; relief of inflammation, pain and edema; relief of neurogenic pain; and bone regeneration, to name a few.

1.5.2 Lasers

LASER, an acronym for *Light Amplification by Stimulated Emission of Radiation*, is defined as any device that emits highly amplified and coherent light (electromagnetic radiation) of a discrete wavelength (monochromatic) (56). The concept of “stimulated emission” was proposed by Albert Einstein in 1916-1917 (57). Stimulated emission is defined as the process by which an electron of an excited atom (or an excited molecular state) will interact with an electromagnetic wave of a certain frequency and may drop to a lower energy level, transferring its energy to that field. By doing so, there is a release

of light energy that is identical to the incoming form of light. A photon, on the other hand, is defined as the quantum of electromagnetic energy. It is regarded as a discrete particle having zero mass, no electric charge, and an indefinitely long lifetime (56). A photon created in this manner has the same frequency and phase as (i.e., coherent with) the stimulating radiation wave (46).

Despite Einstein's early theorization, laser was only physically demonstrated for the first time in 1960, using a ruby laser emitting a red beam of light (51). Since the discovery of lasers, extensive research has been conducted on lasers in order to fully understand their potential for various aspects of daily living. Today, lasers are used in the fields of technology, manufacturing, science, medicine, and dentistry, along with many others (46).

1.5.3 Low Level Laser

Most lasers have high power output and they can generate a significant amount of heat which potentially could have significant negative side effects. The use of LLLT in medicine with an output measured in milliwatts (mW) has gained increasing interest due to its therapeutic effects, while at the same time allowing for less thermal damage than the higher powered lasers (46, 55, 58).

LLLT is also known as soft laser therapy or cold laser therapy. This approach primarily utilizes semiconductor diode lasers that are typically at the red or near-infrared (NIR) parts of the electromagnetic spectrum, and have wavelengths within the range of 630 to 980 nm, depending on the desired effects and the target tissues. These lasers typically have powers ranging from 10-500 mW, and total irradiance of several joules. They do not transmit significant thermal effects to biological tissues (46, 55, 58).

1.5.4 Light emitting diode (LED)

Electrons in a solid material possess two primary energy bands that are located in different positions relative to each other depending upon the material. Valence band (VB) describes a phenomenon whereby the electron exists in bonds and is at a low energy state in a solid matter, while the conduction band (CB) is where the electron exists in a high energy state and acts as a free particle. When an electron is excited to the CB, this leaves behind an empty state that is referred to as a hole. A hole carries a positive charge and behaves like a freed, positive charged entity (59, 60).

According to this relationship between VB and CB, solids are categorized into three categories. Conductors comprise the first category and examples of these include metals whereby the CB and VB overlap forms without a gap, and electrons can freely travel between them. The second category are the insulators and in this group there are significant distances between bands, and a tremendous amount of energy is required to

move electrons from VB to CB; thus, no electric current may be conducted through these materials. The final category are the semiconductors, where VB and CB do not overlap; however, the energy required to move electrons between VB and CB is less than that required for insulators, so that a current can be conducted between them. It is important to appreciate that this current is weaker than that allowed by conductors. The difference between the VB and CB is called band gap (BG), which is the minimal energy required for the electron transition. BG is distinct for each solid material. BG is usually zero for conductors, and is seen to increase in the other two categories of solid materials. A semiconductor is an element that contains both electrons and electron holes. Under the action of an applied field, the hole can move by accepting an electron from a neighboring bond (59, 60).

A light emitting diode (LED) is a device that emits a non-coherent narrow bandwidth (about 5-20 nm) of the electromagnetic spectrum (61, 62). LED devices use semiconducting materials that have a *pn*-junction, which is a contact between two terminals, a p-type semiconductor and an n-type semiconductor. Current flows in the form of electrons from the n-side, which primarily has negative electric charges, to the p-side, which primarily has positive charges. This occurs when sufficient voltage is applied to the semiconductor. Current flow is unidirectional. When the electron reaches the p end, the electron combines with the hole. Due to the movement of electrons to a lower-energy band at the p end, the reaction of a negative and a positive charge yields a quantum of electromagnetic energy that is emitted in the form of a photon of light. This process simply transforms electrical current into light. LED operates on the principle of

spontaneous emission, in which the resultant recombination process between electrons and holes allows for emitted photons in random directions, when excited (48, 59, 60). Spontaneous emission is the process by which an excited atom decays to a state with a lower energy (e.g., the ground state) and emits a photon (46).

The color of the light emitted, or its wavelength, depends on the band gap of the materials forming the p-n junction. LEDs are available at wavelengths ranging from ultraviolet (UV) to visible to near infra-red (NIR) bandwidth (247 to 1300 nm) (48). In photobiomodulation, in order to produce red/NIR wavelengths for the desired effect, gallium arsenide phosphide (GaAsP), gallium arsenide (GaAs), and aluminum gallium arsenide (AlGaAs) are used as semiconductors (46, 52, 63).

1.5.5 LED versus LLLT as a source of photobiomodulation

Laser is distinctively different from ordinary light in many aspects: monochromaticity, coherence, and directionality. Visible light is the sum of multiple colors of the visible spectrum and is usually seen as white. Laser, in contrast, is monochromatic, that is, composed of a single color. The wavelength of light determines whether it is visible or invisible. Laser waves are also coherent; the beam of light is composed of waves, having identical physical size, shape, and direction (46).

LEDs, on the other hand, emit photons via spontaneous emission, as has been previously discussed. The photons are non-coherent, not highly directional, and even though considered by some as monochromatic, they occupy a narrow-band region of the electromagnetic spectrum, rather than having a single wavelength.

Initially, it was thought that coherence of the laser beam was the cause of its therapeutic effect on wound healing. However, research has shown that is not the case (58, 64-66). It was proposed and demonstrated that the therapeutic effect on biological tissues was due to the application of certain wavelengths (64). Further, studies demonstrated that coherence was lost after penetrating superficial layers of skin due to refraction and scattering. Based upon those findings, attempts to replace lasers with partially non-coherent or non-coherent lights were undertaken (48).

While certain characteristics of light have been investigated for their photobiomodulation effects, others remain controversial in the literature, such as the polarization of light and source emission mode. Emission mode, generally speaking, could be either continuous, where emission is at one power level for the duration of the application, or pulsed, where the emission has periodic alternations in power. Pulsed mode emission has short intervals when the emission is terminated between the peaks of emission (46). Most authorities believe that these effects in photobiomodulation are not well understood but it is felt that they do not play significant roles in photobiomodulation (47).

The literature has focused primarily on photobiomodulation's effect using LLL rather than LED. A limited number of articles have discussed the effect of LED on biological tissues. Interest in LED application has increased after NASA's published work on LED describing it as an effective alternative modality to LLL when used to improve wound healing. They investigated the effect of LED on astronauts suspended in zero-gravity conditions who suffered from poor wound healing (61, 62). Results were very promising and these studies argue that it is acceptable to extrapolate scientific findings of LLL studies to explain the mechanisms of action of LED in photobiomodulation (48, 61, 62).

LLLT is currently an accepted therapeutic device in medicine and dentistry; however, it has some disadvantages that render it less practical. LED as a photobiomodulation modality is the most recent studied category of non-thermal light therapies. LED is comparable to LLL, since both have low peak power output, measured in mW, compared to high energy lasers which are measured in watts (W). LED has an additional advantage over lasers as they possess the possibility of combining wavelengths with an array of various sizes, thereby stimulating a broader range of tissue types. LLL has a small optical "footprint" and requires excessive hardware and bulk for the management of large surface areas. On the other hand, LED delivers light over a greater surface area than most lasers and can be used on larger targets, resulting in reduced treatment times. The higher energy density that would be required to treat larger areas with LLL could result in damage to the eye if the retina was unintentionally overexposed. LED does not promote the risk of this type of damage. Phototherapy using LED may therefore be thought of as more practical due to the ability

to produce high efficiency diodes at the desired wavelengths and at reasonable prices (61, 62, 64, 67).

1.5.6 The physics of light-tissue interaction

Depending on tissue's optical properties, light could have four interactions with target tissue. It could be reflected, scattered, transmitted, or absorbed. Reflection occurs when the light is redirected off the surface without producing any effect on the target. Scattering is the process by which photons deviate from their straight direction upon interaction with tissues. Their direction is not predictable, and is not governed by the laws of reflection. Scattering is the primary cause of unwanted thermal damage to adjacent tissues when ablative lasers are used. Transmission occurs when light passes through the tissue without inducing any effect on the target. Transmission is also dependent on the generated light's wavelength. Absorption of light by the target molecules is the desired effect of the phototherapy. It depends on the tissue's water and pigmentation contents as well as the wavelength of the irradiated photons (46, 63).

Different tissues have different optical properties. Skin, mucosa, and bone are transparent, not absorbing light well. On the other hand, muscles have the greatest absorption, primarily due to their high vasculature and hence their high hemoglobin content which is a strong light absorbent (46, 63).

The wavelength of the source combined with the optical properties of the target tissue dictate the penetration depth of light and the dosage at target tissue. The effective or standard penetration depth is defined as the depth at which the fluence, energy per unit area, of light is reduced to 37% of its previous value (68). In the literature, the penetration depth of lasers is also defined by extinction length. Extinction length is defined as the thickness of a substance at which 98% of the energy from the laser is absorbed.

Photons in the red region (600-700 nm) of the electromagnetic spectrum are superficially absorbed while those in the NIR region (780 and 950 nm) penetrate up to 5 cm. The greatest depth of optical penetration is at about 820 nm (46, 63). Wavelengths between 700 and 770 nm are not considered to have much activity.

In order to provide a better understanding of the benefits of photobiomodulation, the next few sections explain the proposed mechanism of action of photobiomodulation at molecular levels.

1.5.7 Mitochondrial ATP production

Adenosine triphosphate (ATP) is the fuel that the cell relies on to perform its normal activities and metabolic reactions, such as transport of substances through membranes, synthesis of chemical compounds, and mechanical work. ATP is a high energy

compound composed of a nitrogenous base adenine, a pentose sugar ribose, and three phosphate radicals. The last two phosphate radicals are connected with the remainder of the molecule with high-energy phosphate bonds. This high-energy bond is very labile, and it can be split whenever energy is required to boost intracellular reactions.

Ninety-five percent of the intracellular ATP production is formed via oxidative reactions in the cellular mitochondria. Pyruvic acid, derived from carbohydrates, fatty acids, and amino acids, is converted at the cytoplasm via glycolysis to Acetyl coenzyme A (acetyl-CoA). Acetyl-CoA then goes through the citric acid cycle, or Krebs cycle.

In the Krebs cycle, acetyl-CoA splits into hydrogen atoms and carbon dioxide. The highly reactive hydrogen atoms yielded combine with oxygen in the mitochondria to release energy. Mitochondrial integral protein enzymes use this energy to convert adenosine diphosphate (ADP) to ATP molecules (69-72).

The majority of hydrogen atoms produced in the Krebs cycle are transferred to coenzymes, NAD^+ and FAD to produce NADH, and $FADH_2$ respectively. The net result of the catabolism of one acetyl-CoA is 3 NADH molecules, 1 $FADH_2$ molecule, and 3 hydrogen ions (H^+) (69).

The mitochondrion is a rod-shaped, double-membraned organelle ranging from 0.5 to 4 micrometers (μm) in length and resides in the cytoplasm of eukaryotic cells. The cell contains about 2,000 mitochondria but their number could vary depending on the cell's

energy expenditure. The mitochondrion has an inner membrane and an outer membrane. The membranes of the mitochondrion divide the organelle into two aqueous compartments, one within the interior of the mitochondrion, called the matrix, and a second between the outer and inner membrane, called the inter-membrane space. The mitochondrion's internal structure is divided into incomplete chambers due to the invagination of the inner membrane forming finger-like projections that are called cristae (47, 70).

The outer mitochondrial membrane is fairly permeable and it contains *porins*, integral protein channels that can undergo reversible closure to control the passage of molecules such as ATP, NAD, and coenzyme A, which are key players in energy metabolism within the mitochondrion. On the other hand, the inner mitochondrial membrane is highly impermeable; molecules and ions require special membrane transporters to gain entrance to the matrix. The inner membrane contains more than 100 different polypeptides and has a very high protein:lipid ratio. The electron transport chain (ETC) is located in the inner mitochondrial membrane (71).

The mitochondrion is involved in many important cellular activities. Aside from its primary role in cellular energy metabolism, it is involved in other activities, such as synthesis of numerous substances, including certain amino acids and the heme groups; regulating calcium (Ca^{2+}) concentration of the cytosol via the uptake and release of calcium ions; and regulating cellular apoptosis (71, 72).

Utilizing the end products of the Krebs cycle, the mitochondrial oxidative phosphorylation pathway is the primary source of ATP production via the ETC, which is primarily composed of cytochromes, iron and copper containing proteins (73).

The ETC is composed of four transmembrane complexes that are embedded in the inner membrane. Three of them are proton pumps: complex I (NADH dehydrogenase), complex III (cytochrome bc1 complex), and complex IV (cytochrome c oxidase). Complex II (succinate dehydrogenase), however, is not a proton pump (47).

The carriers of the ETC are arranged in order of increasingly positive redox potential. Each carrier is reduced by the gain of electrons from the preceding carrier in the chain and is subsequently oxidized by the loss of electrons to the carrier following it (71).

ETC transports two electrons extracted from a combination of an NADH molecule and an H^+, or a single $FADH_2$ molecule. Electrons are transferred from one element of the ETC to the next while losing energy as they move along till the energy-depleted electrons eventually transfer to an oxygen molecule (O_2), which ultimately binds to H^+ to be reduced to water (H_2O) (73).

The redox reactions at the ETC are coupled to conformational changes in electron carriers, the ETC's complexes. As a result, they pump protons from the cytoplasm to the intra-membrane space of the mitochondria, creating an energy gradient that is stored in the form of an electrochemical gradient across the inner mitochondrial membrane.

When protons move back, down their electrochemical gradient, to the cytoplasm through an ATP synthase enzyme, ATP is produced via this coupling mechanism. These last steps are the basics of the chemiosmotic theory which was introduced by Peter Mitchell in 1961. He won the Nobel prize in chemistry later for his work (71, 74).

This process also restores the cell's coenzymes in order to accept more hydrogen atoms from the Krebs cycle (73).

1.5.8 Photobiomodulation mechanism of action (MOA)

The exact mechanism of photobiomodulation is still not well understood. However, many research-driven hypotheses have been proposed since Mester's discovery. The mechanism of action is controversial because the underlying biochemical mechanisms are incompletely understood and parameters used in this field, such as wavelength, fluence, power density, and timing of treatment, are extensively variable.

The optical properties of tissue such as absorption and scattering of light are wavelength dependent. Hemoglobin and melanin have high absorption at wavelengths shorter than 600 nm, while water has high absorption at wavelengths greater than 1150 nm. Due to this, biological tissues have an optical window or range covering the red to NIR wavelengths; effective tissue penetration of light is maximized in the range of 600 to 950 nm of the electromagnetic spectrum (47). Photobiomodulation involves the

application of red to NIR radiation via a LLL or a LED to stimulate cellular function and produce biological and clinical effects (55).

Photons emitted by LLLT or LED device must be absorbed by a molecular chromophore in order to produce a biological effect. Chromophore is a chemical group capable of absorbing light of particular wavelength(s) (71, 72). Each chromophore absorbs light of a specific wavelength. It has been theorized that photobiomodulation is made possible by the activation of cytochrome c oxidase (CCO) at the mitochondrial ETC. CCO, the terminal enzyme at the ETC (complex IV), absorbs light in the red (first absorption peak) to NIR region (second absorption peak) of the electromagnetic spectrum (46, 48).

Karu et al. proposed that CCO is the primary photo-acceptor for the red to NIR range of the electromagnetic spectrum after carrying out action spectra studies on CCO at different oxidation states, observing its biological photoresponse at a variable wavelength, wave number, frequency, or photon energy. They found that the CCO's absorption spectra were similar to the action spectra for biological responses to light in the red to NIR range of the electromagnetic spectrum (65). CCO contains two iron centers and two copper centers (58, 75). It could have a different oxidation or redox state depending on the oxidation state of its four centers. According to the redox state of CCO, each redox state has different absorption spectra. Karu et al. showed four peaks in the LLLT action spectrum at 613.5-623.5 nm, 667.5-683.7 nm, 750.7- 772.3 nm, and 812.5-846.0 nm (75).

Photons at the living tissue can either be absorbed or scattered. Scattered photons will eventually be absorbed or will diffuse away. Once red to NIR photons are absorbed, they interact with CCO within the mitochondria. The quantum of energy delivered by the photon delocalizes electrons in the molecular orbitals of CCO. CCO become excited from the ground state to the first excited state by the quantum of energy delivered by the photon. The energy must be conserved. Three possible outcomes could occur following that event. Heat production via vibration could occur as the excited electron returns to its ground state without emitting a photon. Alternatively, fluorescence could occur when the absorbed photon triggers the emission of another photon with a longer wavelength and less energy, while heat is produced as an energy difference between the absorbed and emitted photons. The last, but not least possible outcome is photochemistry. Multiple photochemical reactions could be seen to occur following the absorption of photon by CCO, such as reactive oxygen species (ROS) formation or the dissociation of a nitric oxide (NO) from its binding site on the CCO (54). Absorption of photons by CCO leads to electronically excited states and, as a result, an acceleration of the mitochondrial ETC occurs (76). Increasing electron transport leads to increased proton pumping and ultimately an increase in ATP production (55, 65).

CCO is inhibited by NO. Mitochondria has a neuronal isoform of NO synthase. NO binds reversibly to CCO. It competes with O_2 for the reduced CCO. NO is believed to play a role in modulating the activity of CCO. It slows cellular respiration in that particular region of the body in order to divert oxygen (O2) to other tissues or cells where it would be needed (47, 77). Karu et al. proposed that NO photodissociation could be another

mechanism via which photobiomodulation could occur. They proposed that LLL could photodissociate NO from CCO. This reverses the inhibition induced by NO binding, and as a result increases the cell's respiration rate (78). Studies have demonstrated that CCO has also a light-mediated nitrite reductase activity that results in an increase in the concentration of NO. It has been demonstrated that NO participates in intracellular signaling pathways as a secondary messenger (54, 78, 79).

Other *in vitro* and *in vivo* studies have demonstrated similar results, while some studies showed that red to NIR light, depending on the parameters of the photobiomodulation source, could decrease NO levels in tissues possibly via inhibiting inducible nitric oxide synthase (iNOS) (80).

It is important to mention that research has demonstrated that photobiomodulation shifts the cell to a more oxidative state. Cells have different redox states during growth, and photobiomodulation could vary according to that. Photobiomodulation is more effective when the cell is in a low oxidation-reduction (redox) stage. Cells at this stage are usually acidic, having a low intracellular pH. Normal and healthy cells at better redox states are not very responsive in that regard (46, 81).

During cellular respiration and ATP production at the mitochondrial ETC, ROS are produced as a by-product. ROS refers to molecules and free radicals, chemical species with one unpaired valence shell electron, and is derived from molecular oxygen. Molecular oxygen contains two unpaired electrons in the outer shell and is not very

reactive. Superoxide anion (O_2^-.) is a relatively stable intermediate for most other ROS. It is a product of the one-electron reduction of molecular oxygen (O_2). Examples of other potent ROS are hydrogen peroxide (H_2O_2), and hydroxyl radical (OH.). ROS could react with nitric oxide (NO.), and other reactive nitrogen species (RNS) as well (77).

Partially reduced and highly reactive metabolites of O_2 may be formed during many redox reactions, such as the reaction at the ETC. Mitochondrial ETC is the primary source of ROS production. Complex I, and complex III of the ETC, in particular, and complex II, to a lesser extent, could leak electrons prematurely to oxygen forming superoxide anion (O_2^-.) (77, 79).

The cell maintains a balanced redox state by balancing between ROS formation and antioxidant defense mechanisms, such as Superoxide dismutases (SOD), enzymes that catalyze O_2^-. dismutation into O_2 and H_2O_2, catalase, and glutathione peroxidases; with these last two enzymes decomposing H_2O_2. Imbalances due to excessive ROS and/or antioxidant defense deficiency lead to oxidative stress that would cause damaging results. ROS, if produced in excess, could haphazardly target cellular components such as proteins, lipids, polysaccharides and DNA. This imbalance has been implicated in many known disease processes (73, 77, 82).

ROS are very potent. Cells such as phagocytic cells, for example, could produce them in large quantities as a part of a host counter-attack defense mechanism. Aside from their reputation as destructive forces, ROS have multiple important cellular roles. For

example, it has been demonstrated that ROS could be a trigger for the intracellular intrinsic pathway of apoptosis. Apoptosis (or programmed cell death) is a vital mechanism used by organisms, for example, to terminate irreparable damaged cells, regulate neuron growth, and modulate the immune system. Failure to regulate apoptosis could lead to catastrophic consequences (71, 72). It has also been demonstrated that ROS play a role in intracellular signaling and cellular regulation (77, 82, 83).

Cell-to-cell communication is crucial for any biological system in order to accomplish the required maintenance of homeostasis and repair in response to injury. Cells participate in extracellular and intracellular communication pathways. Extracellular signals depend on molecules such as growth factors (GFs), cytokines, hormones, and neurotransmitters (NT) that bind to their specific cell surface receptors in a receptor-ligand fashion. This interaction produces signals that propagate intracellularly via multiple variable pathways until the signals reach second messengers, such as cyclic adenosine monophosphate (cAMP) and Ca^{2+}, and by protein phosphorylation cascades. Eventually, signaling pathways lead to the activation of transcription factors that regulate the expression of specific sets of genes that are necessary for diverse cellular activities (83). Transcription factors (TF) are regulatory proteins that bind to specific deoxyribonucleic acid (DNA) sequences in order to modulate the transcription of the encoded genetic information into the messenger ribonucleic acid (mRNA) prior to the ultimate translation of the mRNA into amino acids in order to synthesize proteins required by the cell (70).

ROS signals target other signaling molecules, such as receptor kinases and phosphatases at multiple levels from the cell's surface receptors and all way to the nucleus. ROS has been shown to induce phosphorylation and activation of the PDGF-α, PDGF-β, and EGF receptors, all of which are receptors for important regulatory GFs (83, 84). GFs are structurally related proteins that act either as hormones or as local mediators to regulate a wide range of biological functions such as stimulating cell growth, proliferation, and cellular differentiation (70).

ROS signaling also inhibits the activity of the sarcoplasmic reticulum (SR) Ca^{2+} ATPase (SERCA), an enzyme that rapidly sequesters the Ca^{2+} released into the cytosol back into the SR (85-87). This inhibition results in Ca^{2+} diffusion from SR to the cytosol and leads to an increase in intracellular concentration of Ca^{2+} [Ca^{2+}].

Ca^{2+} concentration inside the cell is normally kept low. Increase in intracellular [Ca^{2+}] can activate or inhibit various enzyme and transport systems, change ionic permeability of membranes, induce membrane fusion, or alter cytoskeletal structure and function. Ca^{2+} functions intracellularly as a second messenger. Ca^{2+} primarily acts in conjunction with a number of Ca^{2+}-binding proteins, such as calmodulin. The Ca^{2+}-binding proteins complex affects many signaling pathways. This complex could bind to a protein kinase, a cyclic nucleotide phosphodiesterase, ion channels, or to the Ca^{2+}-transport system of the plasma membrane. Once bound to a protein kinase, it activates it. The activation of the kinases results in transcription factors phosphorylation and hence, gene transcription

stimulation. One of the most studied targets of ROS is the nuclear factor kappa-light-chain-enhancer of activated B cells (NF-κB) (88, 89).

Nuclear factor kappa-light-chain-enhancer of activated B cells (NF-κB) are a group of transcription factors that can regulate gene expression by binding to discrete DNA sequences. They are present as latent, inactive molecules, and are bound to a family of inhibitory proteins known as inhibitors of NF-κB (IκBs) in the cytoplasm. Phosphorylation of IκB by the IκB kinase (IKK) results in IκB ubiquitination (the process of adding the molecule ubiquitin to a protein in order to tag it for degradation by proteasomes, proteolytic enzymes). This process is followed by IκB degradation. This degradation releases NF-κB. Once NF-κB is liberated, it is translocated into the nucleus where it binds to a specific DNA sequence and activates target gene expression (90-92). NF-κB play an important role in regulating many cellular and organismal processes, such as immune and inflammatory responses, developmental processes, cellular growth and proliferation, and apoptosis.

The action of NF-κB is generally transient, lasting from 30-60 minutes. It is removed from DNA by newly-synthesized IκBa to form a complex that is exported back to the cytoplasm to remain latent again (90-92).

NF-κB activation mostly involves the activation of IKK via a multitude of extracellular signals. The pathway is complex and not fully understood. It also involves other processes such as acetylation, methylation, phosphorylation, and oxidation/reduction.

Some known inducers are oxidative stress agents such as ROS, inflammatory cytokines such as tumor necrosis factor alpha (TNFα) and interleukin 1-beta (IL-1β), viruses and bacterial components such as bacterial lipopolysaccharides (LPS), and ionizing radiation, to name few (91, 92).

In general, it has been proposed that ROS signaling could work via two mechanisms of action.(83) The first mechanism is the alteration in the intracellular redox state.

Cells have many redox couples in order to maintain homeostasis. Examples are nicotinamide adenine dinucleotide (NAD/NADH), nicotinamide adenine dinucleotide phosphate (NADP/NADPH), glutathione/glutathione disulfide couple (GSH/GSSG), and thioredoxin/ thioredoxin disulfide couple ($Trx(SH)_2$/TrxSS). The first molecule of each couple is the oxidized form, while the latter is the reduced form (93).

These alterations in turn activate intracellular cytoplasmic signaling pathways, resulting in transcriptional changes that regulate nucleic acid and protein synthesis. Examples of transcription factors that are regulated by redox state changes are activator protein-1 (AP-1), NF-κB, p53, and hypoxia-inducible factor (HIF)-1 α, an HIF-like factor (94).

Intracellular thiols, primarily GSH and $Trx(SH)_2$, maintain the cytosol in a reduced state. Both proteins are potent antioxidants with a thiol reducing group and they can readily be oxidized, preventing damage caused by ROS. GSH and $Trx(SH)_2$ have high reduced:oxidized ratio by Glutathione reductase (GSR) and thioredoxin reductase (TR),

respectively. It has been shown that both proteins participate in cell signaling via altering their total levels and their oxidized:reduced ratio depending on multiple factors, including ROS activity. For example, decreased GSH levels have been linked to decreased cell proliferation in vascular endothelial cells, increased proliferation of fibroblasts, and inhibition of PDGF receptor autophosphorylation. In the nucleus, studies showed that this redox system is involved in regulating DNA binding to some transcription factors, as well as regulating gene expression in response to oxidant stress. This effect has been implicated in DNA binding of NF-κB (95).

The second mechanism is via oxidative modifications of proteins. By modifying critical amino acid residues, ROS can alter protein structure and function, or regulate their enzymatic activity. The best demonstrated example is the modification of cysteine residues by ROS. By modifying cysteine residues located within the DNA-binding motif of a transcription factor, ROS could alter its ability to bind DNA. An example is the p53 transcription factor. p53 is a tumor suppressor protein. In this model, redox changes of cysteine residues at or near the p53-DNA interface appear to regulate its binding and transactivating potential (96). This has also been implicated as a possible mechanism for EGF-mediated mitogenic signaling (97).

Photobiomodulation may influence the redox potential of target cells as well; a shift in cellular redox potential toward oxidation is associated with the stimulation of cell functions, while a shift toward reduction may be inhibitory (55, 58, 98).

1.6 Applications of photobiomodulation

Photobiomodulation has been implicated in many medical applications. It has been shown to be effective, for example, in wound healing, neural detoxification and regeneration, pain reduction, and bone regeneration.

1.6.1 Role of photobiomodulation in wound healing

Photobiomodulation has been shown to play a significant role in wound healing in multiple animal models and in clinical trials. When LLLT or LED were applied to induced surgical dorsal lesion on diabetic rats, the wounds healed significantly faster than wounds in the control group, in which photobiomodulation was not applied (99). Multiple other animal models with diabetes or without such an intrinsic disease that is known to impair wound healing have shown similar results (61, 62, 67). It has been hypothesized that photobiomodulation speeds the healing process by inducing cytokines and growth factors via one or more of the following effects. Photobiomodulation has been shown to increase cytokines responsible for fibroblast proliferation and migration, increase growth factors inducing fibroblasts collagen synthesis, such as TGF-ß, induce fibroblast transformation into contractile cells, myofibloblasts, in order to speed wound contraction, increase growth factors responsible for the neovascularization, such as VEGF, and last but not least increase cytokines responsible for the inflammatory phase of healing in keratinocytes, such as IL-1 and IL-8 (55, 61, 62, 66, 67).

1.6.2 Role of photobiomodulation in neural protection

Photobiomodulation might play an important role in protecting nerves from damaging neurotoxins. Methanol is converted in the body to formic acid which is known to cause damage to the retina and the optic nerve, leading to blindness. Studies show that brief LED application to rat's retina following methanol intoxication assists in protecting the neural tissue by modulating the effect of this neurotoxin. Other studies also showed that LED application following potassium cyanide (KCN) or tetrodotoxin, both of which are CCO inhibitors, reduced their neural damage and increased the cellular ATP content (100).

1.6.3 Role of photobiomodulation in nerve regeneration

Photobiomodulation effect on nerve regeneration has been researched using primarily LLL. *In vivo* and *in vitro* studies have shown that it stimulates nerve sensory and motor function following injury (101-104).

Using an animal model to test the effect of photobiomodulation post complete resection of sciatic nerve, the LLL irradiated group showed significant increase in axon and fiber diameter, as well as improvement in gait recovery, in a fluence-dependent fashion, in comparison to the control group (102). Similar effects have been seen when transected nerves which were repaired with biodegradable conduits were irradiated with LLL as

well.(105) Histological analysis of irradiated inferior alveolar nerve repaired by means of a conduit also demonstrated increase in post-traumatic nerve regeneration and nerve fiber density in comparison to the non irradiated nerves (106). Similar positive histological results were seen with irradiated crushed facial nerves in an animal model (107).

Clinical studies have shown similar results following application of LLL in patients who had been suffering from incomplete peripheral nerve and brachial plexus injuries for 6 months to several years. Significant improvements in motor function were noticed following LLLT (103). Significant objective and subjective improvement in the distribution of the inferior alveolar nerve following bilateral sagittal split osteotomy was also seen following LLLT in multiple clinical studies (108-110).

The underlying mechanism is not fully understood, but it is postulated that this effect is possibly due to stimulation of migration and fiber sprouting of neuronal cells, Schwann cell proliferation, up-regulating gene expression and secretion of neural factors such as nerve growth factor (NGF), guiding neuronal growth cones possibly via its effect on actin polymerization enhancement at axonal edges (101, 103, 104).

1.6.4 Role of photobiomodulation in pain modulation

Photobiomodulation has an analgesic effect which has been proven in multiple clinical trials. Photobiomodulation has been shown clinically to reduce pain following wisdom

teeth extraction, pain associated with temporomandibular disorders (TMD), pain associated with soft tissue lesion such as oral *lichen planus* and chemotherapy-induced mucositis, and pain associated with orthodontic movement (111-116).

The mechanism by which this happens is not fully understood. It has been shown that high doses of therapeutic light, as discussed in Arndt-Schulz's principle, have inhibitory effects on pain signals. It is proposed that photobiomodulation inhibits pain via multiple mechanisms. It possibly reduces pain by creating transient varicosities along the neurons, which impede signal transmission, modulation of the inflammatory process responsible for pain, opioid-related mechanisms such as production of endogenous endorphins, and alteration of nerve conduction and excitation in peripheral nerves leading to a reduction in the action potential. These effects have also been attributed secondarily to the proposed mechanism of action by which photobiomodulation occur, which was mentioned above, through its effect on the mitochondrial ETC (46, 112, 117).

1.6.5 Role of photobiomodulation bone regeneration and implant healing

Studies conducted primarily using LLLT have suggested that photobiomodulation promotes bone healing, bone mineralization, and bone formation in skeletal defects. Studies have demonstrated that photobiomodulation can regenerate the ATP supply, promote faster angiogenesis that is required for bone regeneration, enhance

mesenchymal cell differentiation into osteoblast, and enhance osteoblast cell attachment and activity (118). Studies have also demonstrated that photobiomodulation, at molecular levels, increased bone nodule formation, ALP expression, osteocalcin, TGF-β, as well as up-regulating other molecules and ions involved in bone regeneration (118-120). It has been also proposed that photobiomodulation modulates the expression of osteoprotegerin (OPG), receptor activator nuclear factor kappa B ligand (RANK), and RANK ligand (RANKL) (15).

In vitro and *in vivo* studies have demonstrated similar stimulatory effects of photobiomodulation around titanium implants (15, 16, 119, 121-127). These studies have represented that photobiomodulation might accelerate endosseous implant healing by the modulation of early cellular attachment and growth on titanium surfaces. These studies imply that by accelerating the process of osseointegration with photobiomodulation, earlier loading of implants could be attempted. No standardized protocol exists for photobiomodulation application as an adjunctive treatment modality to the practice of dental implants placement; however, studies have shown that using a dose of 1-16 J/cm² may have a positive effect on bone metabolism and may be responsible for the aforementioned effects (46, 118, 128). These effects are primarily in the early phases of bone healing following initial bone injury. It has been found that photobiomodulation will likely not produce any effects in late stages of bone regeneration (118).

1.7 Treatment dose

Photobiomodulation as a treatment modality has many independent parameters, making it nearly impossible to establish a standardized dosage protocol for a given indication. It is crucial when evaluating the literature to take into consideration whether the study was conducted *in vitro* or *in vivo*. As well, the effect of photobiomodulation might differ from one species to the next. Thus, it is very important to consider these issues rather than use them by extrapolating their findings and developing parameters for use in clinical practice.

Aside from the wavelength of the light used, as discussed above, effectiveness of photobiomodulation is affected by dosage and treatment duration. A dose of laser energy depends on the number of photons and on its wavelength or color. Energy is inversely related to the wavelength of the laser. For example, red laser has longer wavelength and hence less energy than green laser, while it has more energy than NIR laser (46).

Other important parameters aside from wavelength to take into consideration when applying photobiomodulation are irradiance and radiant exposure. Irradiance is the intensity of light illuminating a given surface. The radiometric unit of measure is W/m^2 or mW/cm^2. Radiant exposure, or energy density, is a function of irradiance and exposure time. It is calculated by dividing the total energy delivered to an area by the area of

irradiation and is expressed as joules per centimeter squared (J/cm²) (46, 63). These parameters could be manipulated by altering the power, exposure time, output mode, and beam area, collectively referred to as external dosimetry parameters. These parameters are limited by the apparatus used. The effect of photobiomodulation depends on internal dosimetry as well. Internal dosimetry depends on the physical characteristics of light upon its interaction with tissue, and the optical properties of the irradiated tissue. Based on this, light could be reflected, transmitted, scattered, or absorbed upon reaching the tissue. This is important in determining the light's penetration depth in order to produce photobiomodulation (46, 63).

Other factors that should be considered in calculating the dose at the target tissue are the distance of the source from the target tissue which primarily affects the light's spot size, as well as whether irradiation is in contact, out of contact, or whether it is applied with pressure on tissue (46, 63).

1.7.1 Biphasic dose response (BDR)

The concept of BDR was introduced by Arndt-Schulz (46, 47). By varying the total delivered light energy density (fluence), photobiomodulation demonstrated such BDR in studies *in vitro* and *in vivo*. Experiments have shown that there is an "optimal window" of light with a lower and an upper threshold to produce its biological effect. Doses lower or

higher than this optimal range will have a diminished therapeutic effect. Higher doses of light might have a negative inhibitory effect (47, 129).

1.8 Limitations of studies in the field of photobiomodulation

There are many limitations in setting a protocol for photobiomodulation which need to be addressed. Photobiomodulation, once doubted by scientists and physicists, has an extensive number of applications, but there is no consensus on definitive protocols for given applications, for many different reasons. First, the mechanism of action on the cellular level is not completely understood. Additionally, there is a shortage of prospective randomized controlled and blinded human clinical trials available in the literature. There are many variable parameters that can be manipulated, as has been previously discussed, such as wavelength, power density, energy density, continuous-wave or pulsed operation modes, pulse parameter, timing of treatment, spot size, and LED versus LLL as a light source. It is difficult to identify two studies in the literature where the same parameters were used (46, 55, 118).

Another issue that certainly complicates a thorough review of the literature is the reported systemic effects of BMP. Aside from the local effect of photobiomodulation at the irradiated site, it has been shown that photobiomodulation might have systemic effects distant from the site of administration (55, 79). This is important to consider when evaluating the literature because some of the studies have demonstrated negative

effects resulting from the use of photobiomodulation when the same subject was used to control a treatment due to these potential systemic, distant effects.

1.9 Goal of study

The application of photobiomodulation in medicine and dentistry requires further extensive scientific research. Randomized clinical trials (RCT) on human participants are the ideal scientific approach to reach valid and reliable conclusions. It has been suggested that photobiomodulation may have a role in enhancing bone regeneration around intraoral endosseous implants during the early phases of healing. Most of these suggestions, however, are concluded from *in vitro* studies (16, 119, 124-127).

The primary purpose of this study was to evaluate the role of photobiomodulation, using an LED device, on the early phases of intraoral endosseous dental implant healing.

Chapter 2: Objective and Hypothesis

2.1 Objective

1) To assess the influence of photobiomodulation in the early bone healing period around dental implants placed in humans

2) To assess the role of photobiomodulation on peri-implant alveolar crestal bone in the early healing period of bone tissue.

2.2. Hypothesis

1) Using LED device, photobiomodulation decreases peri-implant bone resorption in the early phases of osseous healing, and hence decreases the reduction in implant stability seen during the first few weeks after insertion as measured by the Osstell device.

2) Photobiomodulation decreases alveolar crest bone resorption in the early phases of osseous healing around implant.

Chapter 3: Materials and Methods

3.1 Study population

A total of 72 patients requiring 76 dental implants (35 female (F), 37 male (M); mean age 63.5, range 35-100 years) were recruited and consented to participate in this study. This study was approved by both the Research Ethics Board at Mount Sinai Hospital REB #10-0012-E and University of Toronto REB# 24956. All patients requiring intraoral dental implant(s) to replace their missing dentition presented to a dental clinic located in the Greater Toronto Area (GTA). Patients were enrolled in this study between December 2009 and January 2012. A medical history was collected for all participants and clinical and radiographical examinations were performed by a single practitioner. This practitioner was instructed on the appropriate protocol and methods required to standardize the results of this investigation.

The patients were included if they met the following criteria: 1) were able to consent for the surgery; 2) required dental implant(s) to restore missing dentition; 3) did not have any systemic comorbidity including diabetes mellitus, systemic immune disease, or smoking (non-smoking was preferable, but not an absolute); 4) the implant was placed into an alveolar site where the missing tooth was removed at least 3 months previously; 5) the implant site was not previously grafted; 6) the implant surgery was the only procedure performed in the oral region at time of treatment.

Power of study was calculated using an online software provided by Raosoft Inc (130). Sample size required was 377 implants with a confidence interval of 95%. Three

hundred and eighty papers were folded and put in a jar; half of them were designated as control, and the other half as treatment. Participants were randomized to the two groups by drawing a paper from the jar.

Both groups received Nobel Biocare (Nobel Biocare, Gothenburg, Sweden) dental implants, all being placed under local anesthesia. The implants used were either NobelActive, NobelReplace Tapered, or NobelSpeedy Groovy. The control group (Group 1) (n = 47 implants, 46 patients) had their implant placed using the accepted clinical protocols developed by Nobel Biocare for placement of intraoral endosseous root form implants. Following routine placement of implants as in group 1, the treatment group (Group 2) (n = 29 implants, 26 patients) received LED treatment .

3.2 Intraoral implant therapy

After obtaining consent for intraoral dental implant surgery, adequate local anesthesia at the surgical site was obtained through mucosa using an aspirating dental syringe (Integra-Miltex, Pennsylvania, USA). The mucosa at the site of the implant was incised using a #15 Bard Parker surgical blade (Integra-Miltex, Pennsylvania, USA) down to bone. Full thickness mucoperiosteal flaps were reflected from the alveolar ridge crestal bone. Once adequate exposure was obtained, implant site preparation was carried out using surgical drills under copious amounts of saline irrigation, following the manufacturer's recommendations. Sequential drills with increasing diameters were used

to the desired length in order to accommodate the size of the desired implant. The implant was then placed at the prepared site as per the manufacturer's recommendations. Adequate primary stability was obtained clinically. Implant stability was then tested using the Osstell ISQ device immediately following placement. The surgical site was irrigated thoroughly, a healing abutment was placed on the implant, and the surgical incision was closed using 4-0 chromic gut sutures (Hu-Friedy, Chicago, USA)

3.3 LED treatment protocol

While the control group (Group 1) received no further treatment, the treatment group (Group 2) received daily LED treatment according to the treatment protocol described below using the OsseoPulse device (Biolux Research Ltd, Vancouver, Canada) following implant placement (Figure 3.1 a). The protocol used was suggested by the manufacturing company.

The OsseoPulse device consisted of an adjustable headset which could be customized to the patient's face and head. Stability and repeatable positioning were achieved by ensuring three point contacts on the ear and bridge of the nose. This integrated alignment system (Figure 3.1 b) allowed the dentist to position the LED treatment array over the surgical site on the surface of the cheek, ensuring a repeatable positioning by the patient.

The integrated controller (Figure 3.1 c) allowed the operator to prescribe treatment doses. The clinician would adjust, align and fixate the extra-oral LED array on the cheek surface overlying the surgical site and the patient was instructed on how to use the device. The patient then activated the OsseoPulse device at home on a daily basis as prescribed. The OsseoPulse was applied to the surgical site preoperatively for 20 minutes, and for additional 10 daily sessions of 20 minutes each postoperatively starting the day of surgery. The LED device was applied with an energy density of 30 J/cm² per treatment of 20 minutes. Table 3.1 summarizes the parameters of the LED device used in this study.

Table 3.1. Parameters of LED that were used in this study

	Tx
Medium used	LED Semiconductor
Wavelength	620-625 nm
Spectrum	Red
Pulsed or continuous	Continuous wave (cw)
Power density	25 mW/cm² average over surface of array
Energy density (fluence)	30J/cm²
Irradiated area	3.15cm x 1.5cm = 4.73cm^2
Depth of penetration	At mid-alveolus 1-2mW/cm^2
Number of exposures	11
Duration of exposure	20 minutes

(a)

(b)

(c)

Figure 3.1: The OsseoPulse device: (a) The device is in use after being adjusted to patient's face; (b) alignment system; (c) integrated controller that allows the operator to prescribe desired treatment doses. (Images are reprinted with permission from Biolux Research Ltd.: www.bioluxresearch.com)

3.4 Follow-up protocol

Patients were asked to return to the clinic for a follow-up assessment and data collection at 1 week, 2 weeks, 4 weeks, and 8 weeks post-operatively.

3.5 Data collection

The primary care provider, using a data collection form designed by the investigator (Figure 3.2), documented each patient's demographics, and the details of each implant placed including dimensions, location in the oral cavity, and the alveolar bone's quality and ridge type at the implant's site. Quality of alveolar bone was assessed according to Lekholm and Zarb's classification of bone quality, and alveolar ridge type was assessed according to a modified version of Cawood and Howell's classification of residual ridge type (24, 131).

Each implant's primary stability was tested with the Osstell ISQ device at the time of placement. ISQ evaluation was undertaken from the buccal and lingual sides, three times in each location. The average ISQ value was recorded. A post operative peri-apical radiograph of each implant was taken at the day of the surgery, and at every follow-up visit, the primary provider recorded the ISQ value for each implant using the protocol described above.

Another peri-apical radiograph was taken 8 weeks post-operatively. Radiographs were analyzed by a single reader trained to use the image analysis software SigmaScan Pro version 5.0.0 (Systat Software Inc., Chicago, IL, USA). On each postoperative radiograph, crestal bone height immediately in contact with the implant was measured to the apex of the implant on the mesial and distal aspects of the implant. Implant length was measured radiographically as well. The mesial and the distal readings were averaged and this average value was divided by the radiographic length of the implant (Figure 3.3). The outcome was multiplied by 100% in order to obtain the relation of the crestal bone height to the implant length as a percentile value. Implant length used as a radiographic reference. The same measurements were conducted on the radiographs that were taken 8 weeks postoperatively (Figure 3.4). The percentile value obtained at 8 weeks was subtracted from the percentile value obtained from the radiograph taken immediately postoperatively. The mean difference between the control and the treatment groups was analyzed statistically.

PN: 90

Biolux Implant Stability Investigation

Patient's Identification: (#__) _____
Date of Birth: _____/____/_____
Sex: ☐ M ☐ F

Date of implant placement: ____/___/____

Implant Location: _____

Ridge type: (A-E) - Please circle one:

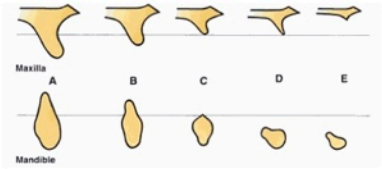

Bone quality (1-4) - Please circle one:

Implant type:

☐ Nobel Biocare (Branemark) _____
☐ Straumann (ITI) _____
☐ Astra (Astratech) _____
☐ Dentsply _____
☐ Zimmer _____
☐ 3i (imlplant innovations inc.) _____
☐ Lifecore Biomedical _____
☐ Imtec _____
☐ Biocon _____
☐ Steri-Oss _____
☐ Biohorizons _____
☐ Other _____

Implant length:

☐ 6 mm ☐ 8 mm ☐ 10 mm ☐ 11.5 mm ☐ 12 mm ☐ 13 mm ☐ 14 mm ☐ 15 mm
☐ Other _____

Implant diameter:

☐ 3.3 mm ☐ 3.75 mm ☐ 4.0 mm ☐ 4.5 mm ☐ 5.0 mm ☐ 5.5 mm ☐ 6.0 mm
☐ Other _____

1

Figure 3.2: Data collection sheet: (a) list of independent variables.

Please record the date and the RFA value:

Immediately post op	Date _____	RFA Value _____
1 week post op	Date _____	RFA Value _____
2 week post op	Date _____	RFA Value _____
4 week post op	Date _____	RFA Value _____
8 week post op	Date _____	RFA Value _____

2

Figure 3.2 (continued): Data collection sheet: (b) ISQ values.

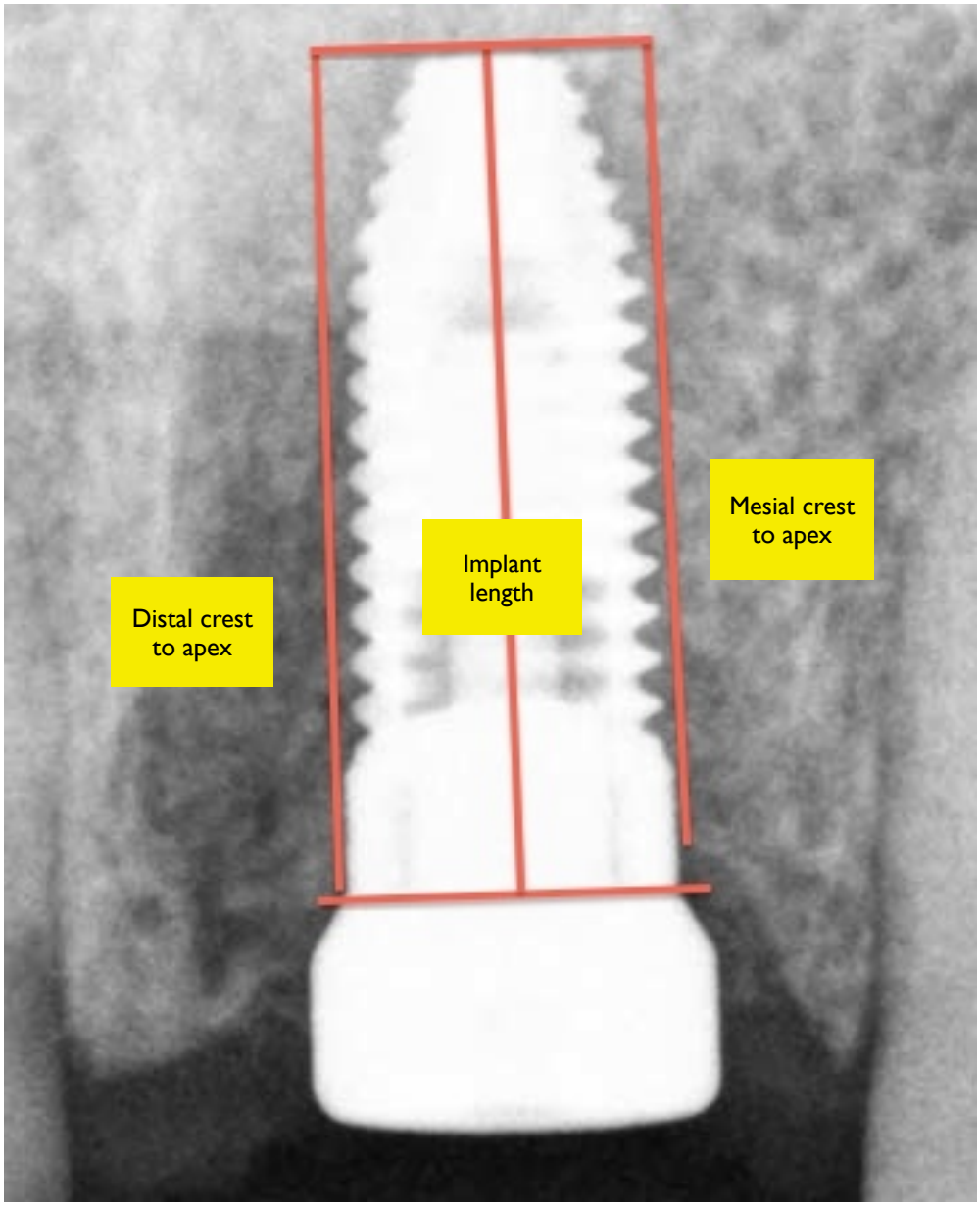

Figure 3.3: Measuring crestal bone height medially and distally in relation to implant length immediately after implant insertion

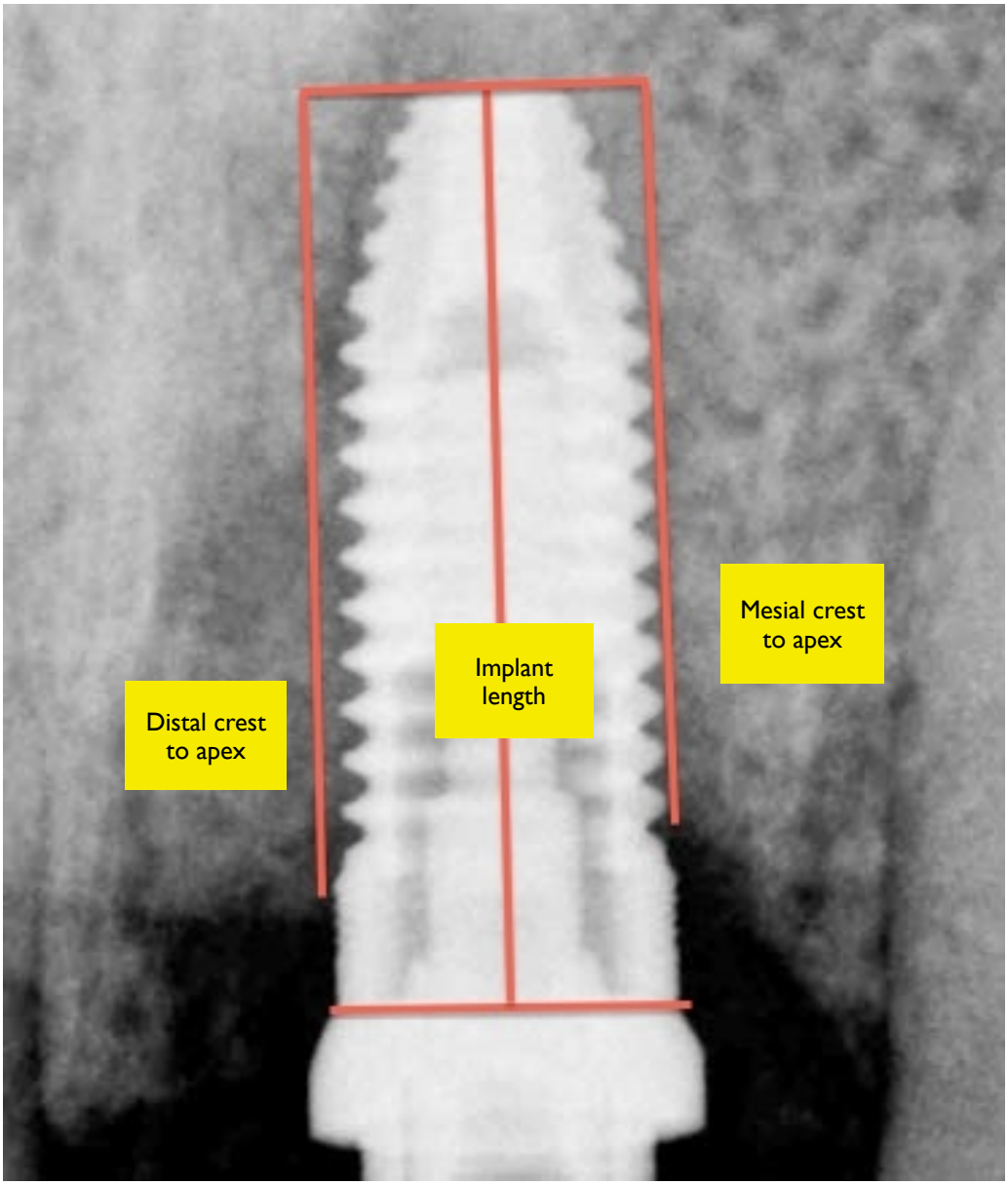

Figure 3.4: Measuring crestal bone height medially and distally in relation to implant length 8 weeks after implant insertion

3.6 Statistical analysis

To measure the effect of LED on the healing of dental implants, the treatment and control groups were compared to each other for changes in the ISQ values. The independent variables, including dimensions, location in the oral cavity, alveolar bone's quality and ridge type at the implant's site, between the two groups were compared statistically as well. A regression analysis was conducted to assess the effect of the independent variables on the ISQ values. Finally, the crestal bone loss was compared radiographically between the two groups. Aside from regression analysis, statistical significance was obtained using Student's 2-tailed T-test and Mann Whitney-U (MWU) test. The data were analyzed using IBM's SPSS for Macintosh, version 20.0.0 (IBM Inc., New York, USA), and Stata (Data analysis and statistical software - StataCorp. 2011. *Stata Statistical Software: Release 12*. College Station, TX: StataCorp LP.) A P value of < 0.05 was considered to be significant. Data are expressed as mean ± standard deviation of mean unless otherwise noted.

Chapter 4: Results

4.1 Introduction

The normality of distribution of the data was assessed for each pair to be compared using a Shapiro-Wilk test. If the data were normally distributed, student's t-test was chosen to assess whether statistical significance existed between the groups. If the data were not normally distributed, the non parametric test Mann Whitney-U (MWU) test was carried out to assess whether statistical significance existed between the groups.
These tests were run on IBM's SPSS for Macintosh, version 20.0.0 (IBM Inc., New York, USA):

1. The independent variables between the two groups, LED group and control group, were statistically analyzed.

2. ISQ values were compared between the groups at each point of time: point zero, 1 week, 2 week, 4 week, and 8 week follow-up.

3. ISQ value change in comparison to point zero, at each point of time, was compared between the two groups.

4. Percentile change in ISQ in comparison to point zero, at each point of time, was compared between the two groups.

5. Change in ISQ, at each point of time, from the previous measurement was compared between the two groups.

6. A regression analysis was performed for the independent variables that were significantly different at point zero using Stata (Data analysis and statistical software - StataCorp. 2011. *Stata Statistical Software: Release 12*. College Station, TX: StataCorp LP.) in order to quantify their contribution to the ISQ value.

7. Crestal bone loss at week 8 in comparison to point zero, was assessed radiographically using image analysis software SigmaScan Pro version 5.0.0 (Systat Software Inc., Chicago, IL, USA) and the difference between the two groups was statistically analyzed using SPSS. Point zero refers to the data obtained immediately after the implant placement.

4.2 Independent variables

4.2.1 Age

Table 4.1. Age comparison between the control and the treatment groups

	Control (n = 46 patients)	Tx (n = 26 patients)
Minimum	38	35
Maximum	100	87
Avg (Average)	64.3	62
StD (Standard deviation)	11.5	12.7
Total Group - Avg 63.49, StD 12.69, p = 0.444 (Student's t-test)		

The age was normally distributed among the subjects. An independent-samples t-test was conducted to compare age difference in LED group and control conditions. There was no significant difference in the scores for LED (Average = 62.0, standard deviation (StD) = 12.7) and control (Average = 64.3, StD =11.5) conditions; t(48.0) = 0.77, p = 0.444. These results suggest that age was not significantly different between the two groups.

4.2.2 Gender

Table 4.2. Gender comparison between the control and the treatment groups

	Control (n = 46 patients)	Tx (n = 26 patients)
Female (F)	26 (57%)	9 (35%)
Male (M)	20 (43%)	17 (65%)
StdDev	0.50	0.49
U = 467.0, p = 0.076 (Mann Whitney U test)		

A Mann-Whitney U test was carried out between the LED group and the control group. The test showed that there was no statistically significant difference between the groups, U = 467.0, p = 0.076.

4.2.3 Implant location in the mouth

Table 4.3. Implant location comparison between the control and the treatment groups

	Control (n = 47 implants)	Tx (n = 29 implants)
Mandible	39 (83%)	15 (52%)
	Posterior (n = 33), anterior (n = 6)	Posterior (n = 11), anterior (n = 4)
	Right (n = 19), left (n = 20)	Right (n = 8), left (n = 7)
Maxilla	8 (17%)	14 (48%)
	Posterior (n = 6), anterior (n = 2)	Posterior (n = 10), anterior (n = 4)
	Right (n = 3), left (n = 5)	Right (n = 9), left (n = 6)
StD	0.40	0.51
Mandible or maxilla: U = 459.5, p = 0.003 (Mann-Whitney U test)		

The two groups were compared statistically in regard to the location of implants (maxilla or mandible). A Mann-Whitney U test was carried out between the LED group and the control group. The test showed that there was a statistically significant difference between the groups, U = 459.5, p = 0.003. The mean rank of the LED group is lower than the mean rank of the control and so the control group had more implants placed in the mandible than the LED group.

4.2.4 Ridge type

Table 4.4. Ridge type at site of implant comparison between the control and the treatment groups

	Control (n = 47 implants)	Tx (n = 29 implants)
Type A	5 (10.64%)	2 (7%)
Type B	30 (63.83%)	18 (62%)
Type C	12 (25.53%)	9 (31%)
Type D	0 (0%)	0 (0%)
Type E	0 (0%)	0 (0%)
StD	0.59	0.58
U = 629.0, p = 0.51 (Mann-Whitney U test)		

A Mann-Whitney U test was carried out between the LED group and the control group. The test showed that there was no statistically significant difference between the groups, U = 629.0, p = 0.51.

4.2.5 Bone quality

Table 4.5. Bone quality at site of implant comparison between the control and the treatment groups

	Control (n = 47 implants)	Tx (n = 29 implants)
Type 1	0 (0%)	0 (0%)
Type 2	45 (96%)	17 (59%)
Type 3	2 (4%)	12 (41%)
Type 4	0 (0%)	0 (0%)
StD	0.2	0.5
U = 428.5, $p < 0.001$ (Mann-Whitney U test)		

A Mann-Whitney U test was carried out between the LED group and the control group. The test showed that there was a statistically significant difference between the groups, U = 428.5, $p < 0.001$. The mean rank of the LED group is higher than the mean rank of the control and so the LED group had worse bone quality than did the control group.

4.2.6 Implant diameter

Table 4.6. Implant diameter (as groups) comparison between the control and the treatment groups

	Control (n = 47 implants)	Tx (n = 29 implants)
Small	3 (6%)	12 (41%)
Medium	12 (26%)	2 (7%)
Large	32 (68%)	15 (52%)
StD	0.61	0.98
U = 501.0, p = 0.026 (Mann-Whitney U test)		
Large ≥ 5 mm; Medium < 5 mm and ≥ 4 mm; Small <4 mm		

A Mann-Whitney U test was carried out between the LED group and the control group. The test showed that there was a statistically significant difference between the groups, U = 501.0, p = 0.026. The mean rank of the LED group is lower than the mean rank of the control and so the LED group had smaller average implant diameter than did the control group.

4.2.7 Implant length

Table 4.7. Implant length (as groups) comparison between the control and the treatment groups

	Control (n = 47 implants)	Tx (n = 29 implants)
Short	16 (34%)	8 (27.6%)
Medium	23 (49%)	13 (44.8%)
Long	8 (17%)	8 (27.6%)
StD	0.86	0.85
U = 625.0, p=0.519 (Mann-Whitney U test)		
Long ≥ 13 mm; Medium <13 mm and >10 mm; Short ≤10 mm		

A Mann-Whitney U test was carried out between the LED group and the control group. The test showed that there was no statistically significant difference between the groups, U = 625.0, p = 0.519. The mean rank of the LED group is higher than the mean rank of the control and so the LED group had longer average implant length than did the control group.

4.2.8 Implant surface

Table 4.8. Implant surface area (as groups) comparison between the control and the treatment groups

	Control (n = 47 implants)	Tx (n = 29 implants)
Small	14 (30%)	13 (45%)
Medium	23 (49%)	10 (49%)
Large	10 (21%)	5 (21%)
No available	0 (0%)	1 (3%)
StD	0.72	0.76
U = 556.0 p = 0.228 (Mann-Whitney U test)		
Large ≥ 250 mm²; Medium <250 mm² and >200 mm²; Small ≤200 mm²		

A Mann-Whitney U test was carried out between the LED group and the control group. The test showed that there was no statistically significant difference between the groups, U = 556.0 p = 0.228. The mean rank of the LED group is lower than the mean rank of the control and so the LED group had less implant surface area than did the control group.

4.3. ISQ averages over follow-up period

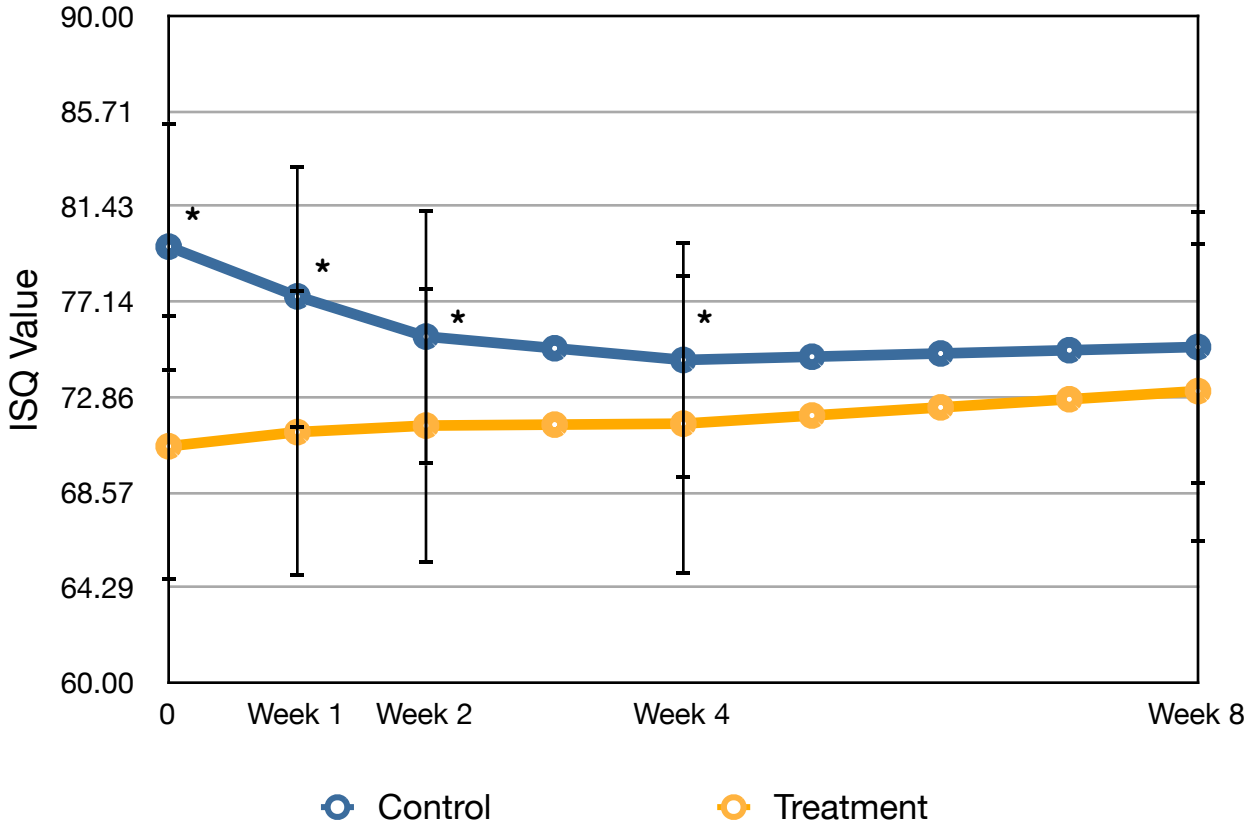

Figure 4.1. ISQ averages over follow-up period (8 weeks). (*) indicates statistical significance. (I) Indicates the standard deviation.

The ISQ data immediately after implant placement at point zero were normally distributed among the groups. An independent-samples t-test was conducted to compare ISQ at point zero in LED group and control conditions. There was a significant difference in the scores for LED (Average (avg) = 70.6, StD = 6.1) and control (Avg = 79.6, StD = 5.7) conditions; $t(56.4) = 6.5$, $p < 0.001$. These results suggest that average

ISQ at point zero was significantly different between the two groups. The average ISQ of the control group was higher than average ISQ of LED group. However, there was no statistically significance difference between the two groups at the end of the 8 week follow-up period ($p = 0.125$).

4.4. ISQ change from initial measurement

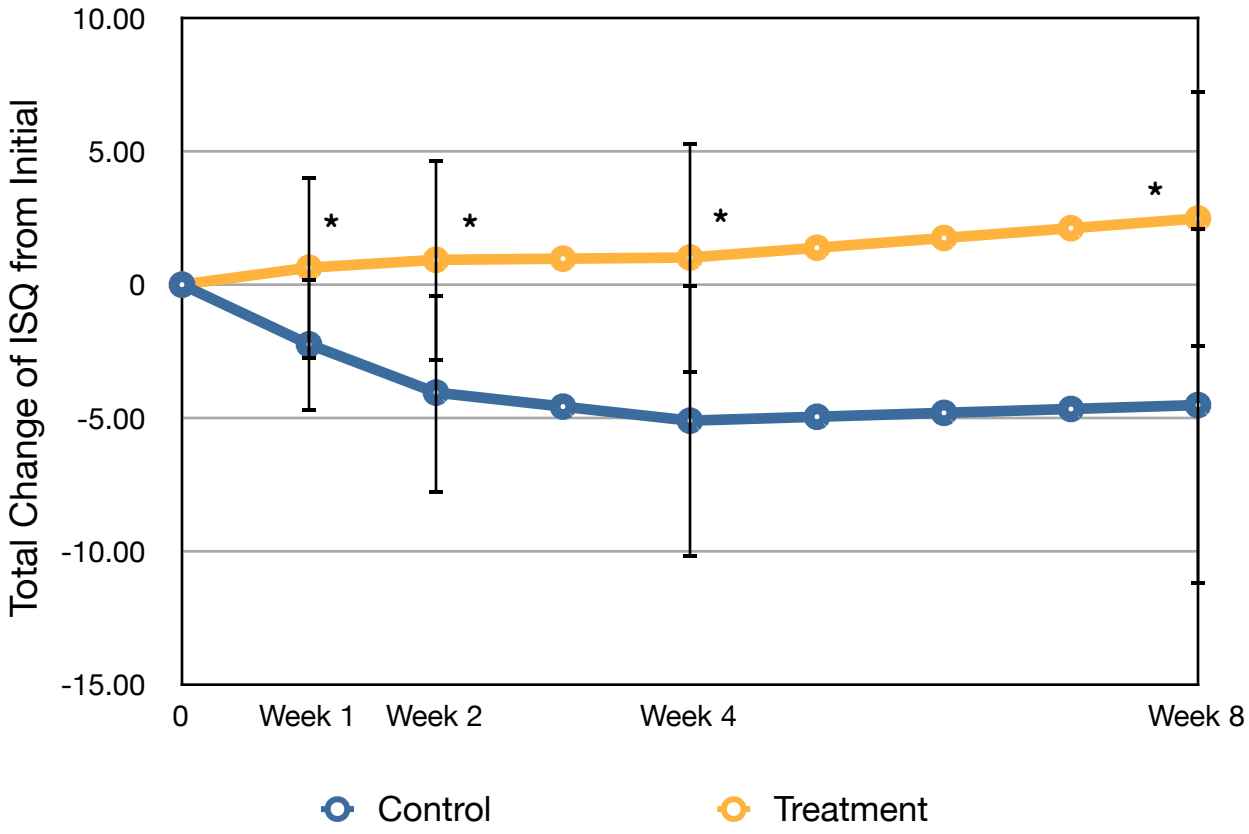

Figure 4.2. Mean total ISQ change from initial measurement. (*) indicates statistical significance. (I) Indicates the standard deviation.

Statistical analysis of change of average ISQ value from average ISQ values at point zero to week 1 (ISQ week 1-ISQ zero), week 2 (ISQ week 1-ISQ zero), week 4 (ISQ week 1-ISQ zero), and week 8 (ISQ week 1-ISQ zero) was carried out between LED group and control group as the following:

At week 1, a Mann-Whitney U test was carried out between LED group and control group. The test showed that there was a highly significant statistical difference between the groups, $U = 265$, $p < 0.001$. The mean rank of LED group is higher than the mean rank of the control and so the LED group had more positive ISQ change from point zero to week 1 than did the control group

At week 2, a Mann-Whitney U test was carried out between LED group and control group. The test showed that there was a highly significant statistical difference between the groups, $U = 209$, $p < 0.001$. The mean rank of LED group is higher than the mean rank of the control and so the LED group had more positive ISQ change from point zero to week 2 than did the control group

At week 4, an independent-samples t-test was conducted to compare ISQ change at week 4 in comparison to point zero in LED group and control conditions . There was a significant difference in the scores for LED (Avg = 1.0, StD = 4.4) and control (Avg = -5.1, StD = 5.2) conditions; $t(67.0) = -5.4$, $p < 0.001$. These results suggest that ISQ change at week 4 in comparison to point zero was significantly different between the two groups and the LED group had a more positive change than the control group.

At week 8, an independent-samples t-test was conducted to compare ISQ change at week 8 in comparison to point zero in LED group and control conditions . There was a significant difference in the scores for LED (Avg = 2.5, StD = 4.9) and control (Avg = -4.5, StD = 6.7) conditions; $t(72.0) = -5.4$, $p < 0.001$. These results suggest that ISQ

change at week 8 in comparison to point zero was significantly different between the two groups and the LED group had a more positive change than the control group.

The above results are summarized in this following table.

Table 4.9. Statistical analysis of mean total ISQ change from initial measurement

	Test	U/t	p
ISQ change week1 - zero	MWU	U = 265	< 0.001
ISQ change week2 - zero	MWU	U = 209	< 0.001
ISQ change week4- zero	Student's t-test	t(67.0) = -5.4	< 0.001
ISQ change week8 - zero	Student's t-test	t(72.0) = -5.4	< 0.001

4.5. ISQ percentile change from initial measurement

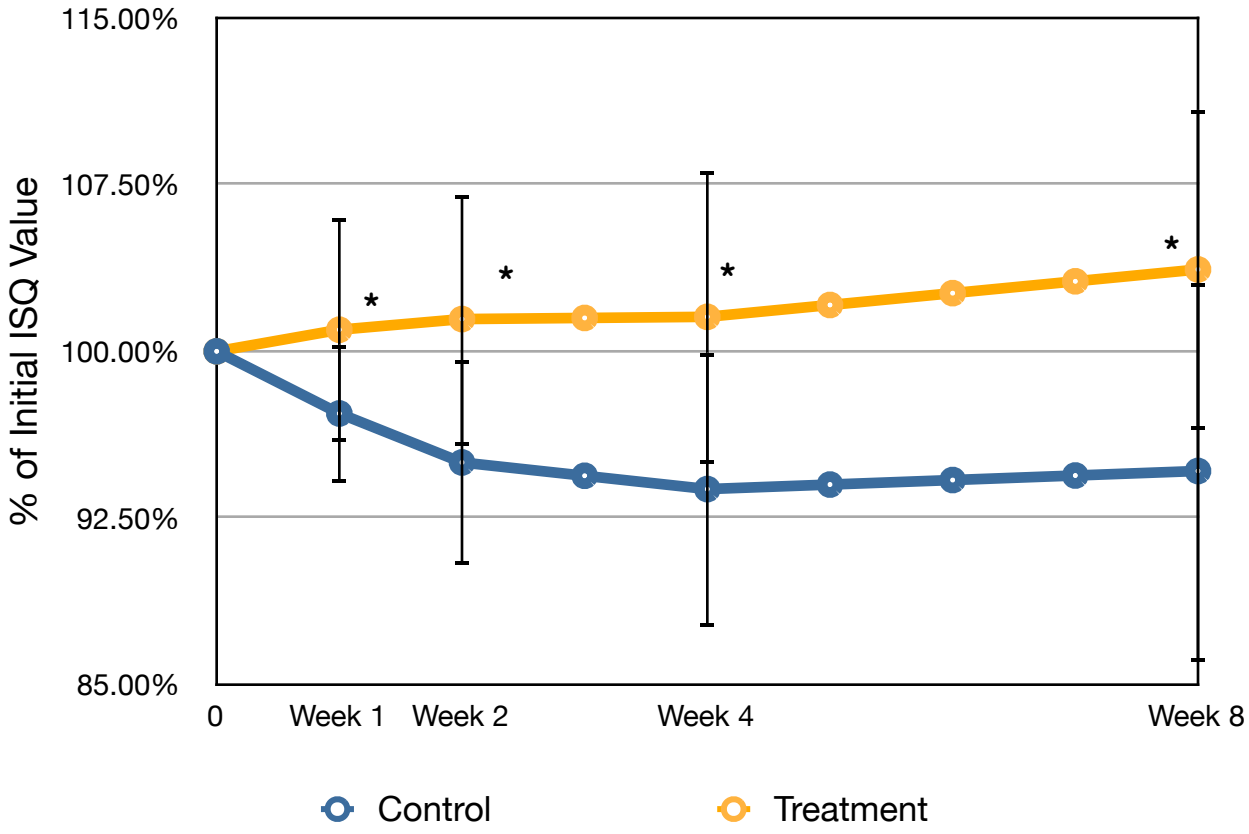

Figure 4.3. Mean ISQ percentile change from initial measurement. (*) indicates statistical significance. (I) Indicates the standard deviation.

Statistical analysis of percentile change of average ISQ value from average ISQ values at point zero to week 1 (ISQ week 1-ISQ zero), week 2 (ISQ week 1-ISQ zero), week 4 (ISQ week 1-ISQ zero), and week 8 (ISQ week 1-ISQ zero) was carried out between LED group and control group as the following:

At week 1, a Mann-Whitney U test was carried out between LED group and control group. The test showed that there was a highly significant statistical difference between the groups, $U = 290$, $p < 0.001$. The mean rank of the LED group is higher than the mean rank of the control and so the LED group had more positive ISQ percentile change from point zero to week 1 than did the control group.

At week 2, a Mann-Whitney U test was carried out between LED group and control group. The test showed that there was a highly significant statistical difference between the groups, $U = 223.5$, $p < 0.001$. The mean rank of LED group is higher than the mean rank of the control and so the LED group had more positive ISQ percentile change from point zero to week 2 than did the control group.

At week 4, a Mann-Whitney U test was also carried out between LED group and control group. The test showed that there was a highly statistical significant difference between the groups, $U = 249.5$, $p < 0.001$. The mean rank of LED group is higher than the mean rank of the control and so the LED group had more positive ISQ percentile change from point zero to week 4 than did the control group.

At week 8, a Mann-Whitney U test was also carried out between LED group and control group. The test showed that there was a highly statistical significant difference between the groups, $U = 244.5$, $p < 0.001$. The mean rank of LED group is higher than the mean rank of the control and so the LED group had more positive ISQ percentile change from point zero to week 8 than did the control group.

Previous results are summarized in the following table.

Table 4.10. Statistical analysis of mean ISQ percentile (%) change from initial measurement

	Test	U/t	p
ISQ% change week1 - zero	MWU	U = 290.0	< 0.001
ISQ% change week2 - zero	MWU	U = 223.5	< 0.001
ISQ% change week4- zero	MWU	U = 249.5	< 0.001
ISQ% change week8 - zero	MWU	U = 244.5	< 0.001

4.6. ISQ change from previous measurement

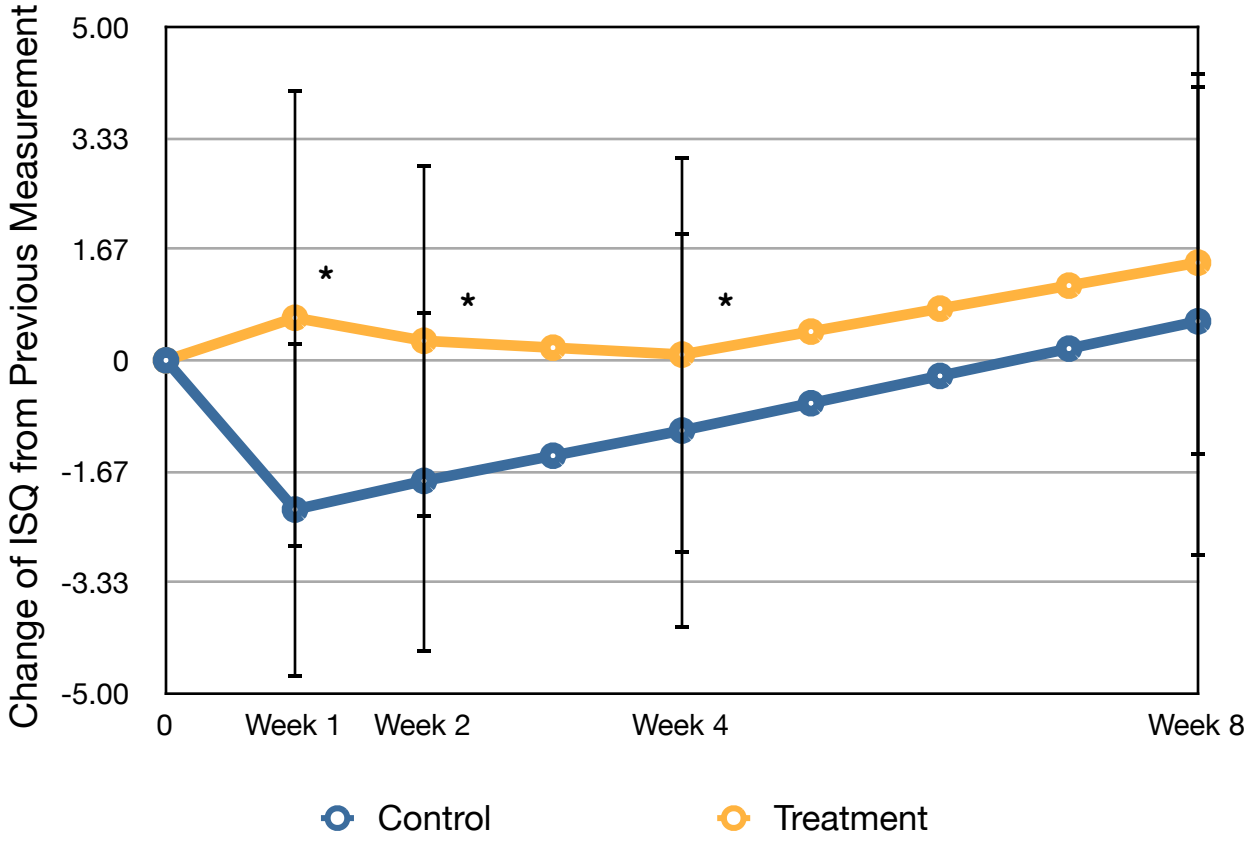

Figure 4.4. Mean change of ISQ from previous measurement. (*) indicates statistical significance. (I) Indicates the standard deviation.

Statistical analysis of change of average ISQ value from average ISQ values at previous measurement was carried out between LED group and control group as the following:

At week 1, a Mann-Whitney U test was carried out between LED group and control group. The test showed that there was a highly statistical significant difference between the groups, $U = 290$, $p < 0.001$. The mean rank of LED group is higher than the mean rank of the control and so the LED group had more positive ISQ percentile change between week 1 to point zero than did the control group.

At week 2, a Mann-Whitney U test was carried out between LED group and control group. The test showed that there was a highly statistical significant difference between the groups, $U = 322.0$, $p < 0.001$. The mean rank of LED group is higher than the mean rank of the control and so the LED group had more positive ISQ change between week 2 and week 1 than did the control group.

At week 4, a Mann-Whitney U test was carried out between LED group and control group. The test showed that there was a highly statistical significant difference between the groups, $U = 496.0$, $p = 0.047$. The mean rank of LED group is higher than the mean rank of the control and so the LED group had more positive ISQ change between week 4 and week 2 than did the control group.

At week 8, a Mann-Whitney U test was carried out between LED group and control group. The test showed that there was no statistical significant difference between the groups, $U = 531.0$, $p = 0.104$. The mean rank of LED group is higher than the mean rank of the control and so the LED group had more positive ISQ change between week 8 and week 4 than did the control group.

Previous results are summarized in the following table.

Table 4.11. Statistical analysis of mean ISQ change from previous measurement

	Test	U/t	p
ISQ change week1 - zero	MWU	U = 290.0	< 0.001
ISQ change week2 - week1	MWU	U = 322.0	< 0.001
ISQ change week4- week2	MWU	U = 496.0	0.047
ISQ change week8 - week4	MWU	U = 531.0	0.104

4.7 Regression analysis of the independent variables at point zero

Regression analysis for the independent variables documented in the study at point zero was carried out using Stata. The regression analysis included all the independent variables previously mentioned (Section 4.2) except the alveolar ridge type. This was excluded because available bone quantity, from a practical perspective, is better represented by the implant dimensions. Only 75 implants were included out of the total 76 implants, because the surface area of one of the implants was not provided by manufacturer.

Table 4.12. Regression analysis of independent variables affecting ISQ at point zero

At ISQ point zero	Coef	p
Age	0.04	0.461
Sex	1.49	0.184
Implant location (maxilla in relation to mandible)	-1.51	0.267
Bone quality	-6.10	0.001
Implant diameter (small in comparison to large)	-7.25	0.002
Implant diameter (medium in comparison to large)	-2.13	0.226
Implant length (small in comparison to large)	-2.27	0.233
Implant length (medium in comparison to large)	0.22	0.889
Implant surface (small in comparison to large)	-0.08	0.975
Implant surface (medium in comparison to large)	-2.59	0.132

The regression analysis shows that bone quality and implant diameter (small when compared to large and vise vera) have a statistically significant effect on the ISQ value at point zero. For every numerical increase in the bone quality according to the Lekholm-Zarb classification, the ISQ value decreases by 6.10 (24). For changing the diameter of the implant from large group to small group, the ISQ value of the implant decreases by 7.25, and vice versa.

4.8 Timing the effect of photobiomodulation during the of peri-implant healing period

Using a change model, multiple regression analyses were conducted to establish the exact period of the implant healing during which the photobiomodulation seem to be effective. Effectiveness is assessed by measuring the independent variable in this model, which is the change in the ISQ value from the previous reading. The dependent variable is the use of the OsseoPulse device to induce photobiomodulation. Independent variables in the previous table (Table 4.12) were also included in this model; however, they have been omitted in the following table (Table 4.13) for simplicity.

Table 4.13. Timing the effect of photobiomodulation during the of peri-implant healing period using a regression analysis in a change model

Independent variable	Coef	p
ISQ change week1 - zero	2.29	0.025
ISQ change week2 - week1	1.48	0.053
ISQ change week4- week2	0.67	0.495
ISQ change week8 - week4	0.48	0.617
ISQ change week8 - zero	3.23	0.102
ISQ change week8 - week1	2.31	0.178
ISQ change week8- week2	1.16	0.383
ISQ change week4 - zero	3.00	0.055
ISQ change week4 - week1	1.83	0.160

This model shows that the photobiomodulation effect on implant stability as measured by ISQ is statistically significant during the following periods: point zero to week 1, week 1 to week 2, and point zero to week 4. However, analyzing the first four weeks further shows that the photobiomodulation effect doesn't seem to be statistically significant during the following periods: week 1 to week 4, and week 2 to week 4. From these results, it could be concluded that the photobiomodulation effect is statistically significant during the first two weeks of healing, and the effect seen on the period from point zero to week 4 most likely is due to the statistically significant effect seen during the first two weeks.

4.9 Radiographic analysis of crestal bone loss

Table 4.14. Crestal bone percentile changes at 8 weeks

	Control	Tx
Number of implants	14	13
Average bone loss	-11.87%	-5.22%
StD	7.97%	8.86%
p = 0.05 (Student's t-test)		

The data were normally distributed among subjects. An independent-samples t-test was conducted to compare crestal bone loss in LED group and control conditions. There was a significant difference in the scores for LED (Avg = - 5.2, StD = 8.9) and control (Avg = -11.9, StD = 8.0) conditions; t(24.2) = -2.05, p = 0.05. These results suggest that crestal bone loss was significantly different between the two groups. The mean crestal bone loss among the control is significantly more than the LED at 8 weeks.

Chapter 5: Discussion

5.1 Introduction

The primary purpose of this study was to evaluate the effect of the OsseoPulse device in the early phases of intraoral endosseous implant healing using a RCT on human participants. The dependent variable was implant's ISQ value, which was assessed using the Osstell ISQ device. The crestal bone percentile loss was evaluated on digital peri-apical radiographs.

5.2 Independent variables at point zero

Eight independent variables that were thought could affect the results directly or indirectly were investigated: age, gender, jaw (mandible or maxilla), bone quality, ridge type, implant diameter, implant length, and implant surface. The implants were classified according to each dimension (length, diameter, and surface) and then were grouped into small, medium, and large categories. When comparing the two groups, only three (bone quality, implant diameter, and implant location) of the eight evaluated, were found to be statistically different. Of the three independent variables, only the bone quality and implant diameter were likely to have an effect on total implant stability and the primary stability of implants.

5.3 Implant stability at point zero

All implants placed in this study had adequate primary stability at the beginning of the study and immediately after insertion of implants as measured by the Osstell device. The lowest ISQ recoded at point zero was 61. Studies have demonstrated that implants with ISQ values above 54 to 60 are considered to be stable (40-43, 45). However, the mean ISQ value of the control group was significantly higher than that of the treatment group at point zero.

As mentioned in the introduction, the primary stability of implants is a result of the biomechanical interlocking of the implant and the bone tissue and it can be dependent primarily upon four factors: surgical technique, implant design, bone quantity, and bone quality (22, 26, 31, 34).

1. All implants were placed by a single operator following a standard surgical protocol. A single operator who is experienced with implant surgery and with the application of the OsseoPulse device reduces or eliminates the risk of inter-operator variability. As the operator was highly experienced in placing implants and utilizing the OsseoPulse device prior to this study, the risk of intra-operator variability was eliminated.

2. All implants used in this study were manufactured by Nobel Biocare. They all were produced from chemically unchanged variants of commercially pure titanium and shared the same surface micro-topography and surface chemistry (132). Previous

studies have demonstrated that these characteristics do not affect primary stability, yet they enhance bone formation and hence hasten the process of osseointegration (22, 26).

The implants used in this study had different dimensions (length, diameter, and surface area) as dictated by the amount of alveolar bone available at the implant site. The direct effect of implant dimensions on primary stability is not well defined in the literature. Bischof et al. found that using implants with different diameters or lengths did not affect primary stability as tested using RFA technology (133). On the other hand, other studies have demonstrated that using implants with larger diameter increases the primary stability of dental implants as they engage more cortical bone (134, 135). Kessler-Liechti et al. demonstrated this direct correlation of implant and implant stability using RFA technology (136). The data from this study suggest that implant diameter, as tested by the Osstell device, was directly related to the primary stability of implants. The two groups had statistically significant differences in implant diameters at the beginning of the study and the average diameter of the control group implants was higher than that of the treatment group. To relate the effect of this difference to the difference in ISQ values between the two groups at time zero, a regression analysis was conducted. The test showed that there is a statistically significant correlation between implant diameters and ISQ value at this time point. This correlation was positive; for every increase in implant diameter from small to large implant diameter, as grouped in the results section, there is an increase in ISQ value at point zero by 7.25. There was no statistically significant difference between

the two groups in the length and surface area of the implants. Regression analysis did not show any significant correlation between these parameters and implant primary stability either. In conclusion, It seems that implant diameter is the only implant-related independent variable that might significantly affect the obtained ISQ values in this study.

3. Bone quantity was assessed using a modified version of Cawood and Howell's classification of residual alveolar ridge type (131). There were no statistically significant differences between the two groups with respect to the alveolar ridge type.

4. Lekholm and Zarb developed a classification system for alveolar ridge bone quality in the 1980s. They classified alveolar ridge bone quality into four categories according to the proportion of cortical and cancellous bone. According to this classification, class I bone, which is mostly located in the anterior mandible, has the highest cortical to cancellous proportion while class IV has the lowest cortical to cancellous bone proportion (24). Cortical bone has higher density of mineralized lamellae and is more compacted in comparison to trabecular bone. In essence, there is more available compact bone in contact with the implant, and hence, this increases the bio-mechanical locking required to obtain optimal primary stability (22).

Our data demonstrated that the primary stability of implants could be directly related to bone quality as evaluated using the Osstell device. The two groups had statistically significant differences in bone quality at the sites of implants at time zero; mean

diameter size of the control group was higher than that of the treatment group. To relate the effect of this difference to the difference in ISQ values between the two groups at point zero, a regression analysis was conducted. This analysis showed that there was a statistically significant correlation between bone quality and ISQ value at this point in time. This correlation was positive; for every increase in implant diameter from small to large implant diameter, as grouped in the results section, there was an increase in ISQ value at point zero by 7.25.

5.4 Implant stability change over 8 weeks

The literature suggests that we should expect a continuous decrease in implant stability over the first few weeks after implant placement, prior to witnessing an increase in the stability. The early decrease in primary stability of the implant is due to the osteoclastic activity around the implant-to-bone contact areas, while the latter gain in stability is due to the new bone formed around the implant surface as a part of the osseointegration process. There is a critical period that has been estimated to be 2 to 3 weeks following implant placement, and during which the implant stability might be compromised, prior to gaining an adequate secondary stability (33, 35). Elimination or reduction of this dip in the implant stability has been the target of researchers and clinicians, especially with the introduction of the concepts of early and immediate implant loading. Such efforts to enhance osseointegration primarily have targeted implant surface characteristics such as surface topography and surface chemistry, as well as the environment around the

dental implant. In this category, attempts are being made in order to provide optimal conditions for implant integration by the incorporation of exogenous influences such as growth factors, gene therapy, and photobiomodulation using a low level laser therapy (LLLT) or light emitting diode (LED) (5-12).

In the study presented in this thesis, the control group showed similar changes in the stability curves as seen in other studies. There was a decrease in the ISQ values in the first weeks following implant placement. The decrease continued for four weeks prior to increasing. On the other hand, the treatment group did not demonstrate this dip in stability; instead, there was a continuous increase in stability as reflected by measuring ISQ values over the 8 week follow-up period. Despite the statistically significant difference in primary stability between the two groups at the beginning of the study, there was no statistical significance in ISQ values, and hence stability between the two groups by the end of the follow-up period (8 weeks).

It is important to mention that although the implants in the control group had an early decrease in stability, the mean ISQ values of these implants were at all times well above the critical ISQ value of 54 to 60 required for implant survival (40-43, 45).

5.5 The effect of photobiomodulation

The effect of Photobiomodulation may be explained by reviewing the proposed mechanisms of action. Oxygen tension is an important factor in determining the fate of mesenchymal cells involved in the early phases of peri-implant tissue healing. Depending on oxygen tension, mesenchymal cells can differentiate into fibroblasts, chondrocytes, or osteoblasts (5). Bone injury induced by implant site preparation for example, leads to localized tissue hypoxia, and deprivation of ATP supply necessary for bone metabolism at the injury site (4). Studies have shown that photobiomodulation can have a effect on the cell membrane and mitochondria resulting in regenerating the cellular supply of ATP and increasing RNA and DNA synthesis. These changes promote the release of growth factors and cytokines, enhance mesenchymal cell differentiation into osteoblasts, enhance osteoblast cell attachment and activity, promote faster angiogenesis, enhance collagen formation, increase calcium phosphate production, and ultimately increase bone matrix production and mineralization (118). The results in promotion of bone regeneration will enhance and speed up dental implant integration in the early healing phases following their placement (15, 16, 118, 119, 121-127). This is consistent with previously conducted *In vitro*, *in vivo,* and clinical studies.

The results of this investigation concur with the findings of other studies reported in the literature. Statistically significant differences were seen between the treatment and the control groups with respect to the ISQ values from time point zero to week 1, week 1 to week 2, and week 2 to week 4. A regression analysis of these data designed to

correlate the effect of photobiomodulation on these results showed that the effect of photobiomodulation was statistically significant only during the first two weeks of healing. These findings support the hypothesis that the expected effect of Photobiomodulation will be seen primarily during the first two weeks following implantation.

5.6 Photobiomodulation effect on crestal bone loss

A crestal bone resorption is expected following implant placement. The process of resorption is multi-factorial and is dependent on the amount of surgical trauma, the preservation of biological width, the reaction of surrounding tissues to insults, the design of implant components, and the implant position in relation to the crest and adjacent anatomical structures (26, 137-139). Researchers and clinicians have attempted to develop methods to decrease this loss by improving implant design, improving implant surface microtopography, changing implant-abutment connectors, and by platform switching (137, 140-143).

To our knowledge, the effect of photobiomodulation on the early crestal bone loss around implants has not been investigated. This study may be considered to be a pilot study, considering the small sample population (n = 27 implants; control group = 14 implants, and treatment group = 13 implants). Standardized protocol to obtain peri-apical radiographs was not followed. Angulation of the radiographs was variable and

very limited number of radiographs had reasonable angulation to be analyzed. However, from the limited number of obtained radiographs, the crestal bone adjacent to the implant surface at 8 weeks follow-up was compared to those obtained immediately after implant insertion. The data demonstrated a statistically significant difference among the two groups. There was less decrease in crestal bone height in the treatment group as compared to the control group.

5.7 Study limitations

Analyzing this clinical trial retrospectively, multiple limitations were encountered.

1. The design of the study was changed after the beginning of the trial. The initial study design was to compare patients who will be treated within the University of Toronto and patients who will be treated by dentists in the community. The study design was explained thoroughly to the practitioners who intended to participate in the study in multiple training sessions prior to commencing this clinical trial. However, none of the participating dentists followed the protocol except one. The study also intended to assess the analgesic effect of the OsseoPulse device. Patients were supposed to document their pain level following implant placement using a visual analogue scale (VAS) as well as documenting the analgesic medications they were taking post-operatively. These data were not documented adequately to be presented in this study. Within the University of Toronto, there was a lack of sufficient number of

patients to meet the exclusion criteria as most of implants' sites were previously grafted.

2. Sample population size was small. Power of study was calculated. Sample size required was 377 implants with a confidence interval of 95%. However only 76 implants were included.

3. The study lacked an on-site coordinator. All practitioners prior to commencing the study received adequate training regarding the study protocol, however an on-site coordinator would have ensured that protocol was followed properly.

4. The study is not blinded in many aspects. The dentist who placed the implants measured the ISQ values as well. The dentist was not blinded about whether patients were in the control or the treatment groups. Patients were not blinded either. Patients in the control group could have received a sham-irradiation using a device that looked similar to the OsseoPulse device.

5. Standardized protocol to obtain peri-apical radiograph post-operatively was not used by the practitioner. Most radiographs were severely angled, missing apical portion of implant, or had significant artifact effect that negated their value for the intended analysis. As a result, only 27 implants were included in the radiographic analysis of crestal bone out of the 76 implants that were included in the ISQ analysis. The approach used in this study to analyze the crestal bone height is not ideal. Using a

perpendicular radiograph at an equal distance from the implants using a stent would have resulted in an accurate measurement of the crestal bone height change in millimeters rather than a percentile value.

5.8 Future directions

In the future, RCT could involve projects with larger population sizes, decreasing the possible effect of the independent variables and increasing the power of the study.

In addition, histological studies using animal models would assist in the appreciation of the effects of photobiomodulation on the early phases of endosseous implant healing. With the use of animal models such as those used by Buser et al. or Berglundh et al., histological studies could be conducted after sacrificing the subject animals at different time intervals. This will allow for evaluation of the early osseous healing events around implants. It can also be used to assess bone-to-implant contact (BIC) during these periods in order to be able to quantify the effect of photobiomodulation 3-dimensionally (7, 35).

It would also be interesting to determine the effect of photobiomodulation on endosseous intraoral implants placed into fresh extraction sites, immediately following tooth removal, as well as implants placed into augmented bone (autogenous, allogenic, or xenogenic.)

Chapter 6: Conclusion

In conclusion, from this investigation, there is a suggestion that the use of LED around dental implants will allow for a continuous increase in ISQ value and may reduce crestal bone resorption in the early phases of bone healing around dental implants. However, further evaluation of this technology is required in a larger trial with a larger sample size, better coordination and control, a standardized radiograph protocol, and supplemented with *in vivo* histological studies. These are needed in order to develop a better understanding of photobiomodulation with the aim to promote a better endosseous implant-based clinical practice.

References

1. Block MS, and John S. Kent. Endosseous implants for maxillofacial reconstruction. Philadelphia: W.B. Saunders, 1995.
2. Branemark PI, Hansson BO, Adell R, Breine U, Lindstrom J, Hallen O, et al. Osseointegrated implants in the treatment of the edentulous jaw. Experience from a 10-year period. Scand J Plast Reconstr Surg Suppl 1977;16:1-132.
3. Albrektsson T, Johansson C. Osteoinduction, osteoconduction and osseointegration. Eur Spine J 2001;10:S96-101.
4. Brånemark P-I, George A. Zarb, and Tomas Albrektsson. Tissue-integrated prostheses: osseointegration in clinical dentistry. Chicago: Quintessence, 1985.
5. Schwartz Z, Boyan BD. Underlying mechanisms at the bone-biomaterial interface. J Cell Biochem 1994;56:340-347.
6. Cochran DL, Buser D, ten Bruggenkate CM, Weingart D, Taylor TM, Bernard JP, et al. The use of reduced healing times on ITI implants with a sandblasted and acid-etched (SLA) surface: early results from clinical trials on ITI SLA implants. Clin Oral Implants Res 2002;13:144-153.
7. Buser D, Broggini N, Wieland M, Schenk RK, Denzer AJ, Cochran DL, et al. Enhanced bone apposition to a chemically modified SLA titanium surface. J Dent Res 2004;83:529-533.
8. Schwarz F, Herten M, Sager M, Wieland M, Dard M, Becker J. Histological and immunohistochemical analysis of initial and early osseous integration at chemically modified and conventional SLA titanium implants: preliminary results of a pilot study in dogs. Clin Oral Implants Res 2007;18:481-488.
9. Spagnoli DB, Marx RE. Dental implants and the use of rhBMP-2. Dental clinics of North America 2011;55:883-907.
10. Yan MN, Tang TT, Zhu ZA, Zhou XS, Jia QW, Yu CF, et al. [Effects of bone morphogenetic protein-2 gene therapy on the bone-implant interface: an experimental study with dogs]. Zhonghua Yi Xue Za Zhi 2005;85:1521-1525.
11. Cao YG, Wang R, Song K, Xiong ZQ, Du JM, Wang HJ. [Effects of transforming growth factor-beta1 gene therapy on bone rarefaction around endosseous implant]. Hua Xi Kou Qiang Yi Xue Za Zhi 2007;25:335-338.
12. Chang PC, Seol YJ, Cirelli JA, Pellegrini G, Jin Q, Franco LM, et al. PDGF-B gene therapy accelerates bone engineering and oral implant osseointegration. Gene Ther 2010;17:95-104.
13. Brawn P K-HA. Accelerating implant stability after LED photobiomodulation treatment. Europian Assoc Osseointegration, 2007.
14. Brawn P K-HA, Boeriu S and Clokie CM Accelerated Implant Stability After LED Photobiomodulation. J Dent Res 2008;87:2021.
15. Kim YD, Kim SS, Hwang DS, Kim SG, Kwon YH, Shin SH, et al. Effect of low-level laser treatment after installation of dental titanium implant-immunohistochemical study of RANKL, RANK, OPG: an experimental study in rats. Lasers in surgery and medicine 2007;39:441-450.
16. Khadra M. The effect of low level laser irradiation on implant-tissue interaction. In vivo and in vitro studies. Swed Dent J Suppl 2005;172:1-63.

17. Davies JE. Bone engineering. Toronto: EM. Squared, 2000.
18. Brånemark P-I. The osseointegration book: From calvarium to calcaneus. Berlin: Quintessence, 2005.
19. Davies JE. Bone interface group. 2012.
20. Davies JE. Mechanisms of endosseous integration. Int J Prosthodont 1998;11:391-401.
21. Davies JE. Understanding peri-implant endosseous healing. J Dent Educ 2003;67:932-949.
22. Jokstad A. Osseointegration and dental implants. Ames, Iowa: Wiley-Blackwell, 2009:xxiii, 419 p.
23. Cooper LF. Biologic determinants of bone formation for osseointegration: clues for future clinical improvements. J Prosthet Dent 1998;80:439-449.
24. Lekholm U ZG. Patient selection and preparation. In: Tissue-Integrated Prostheses: Osseointegration in Clinical Dentistry. Chicago: Quintessence, 1985.
25. Marx RE. Bone and bone graft healing. Oral Maxillofac Surg Clin North Am 2007;19:455-466.
26. Davarpanah M. Clinical manual of implant dentistry. London: Quintessence, 2003.
27. Buser D, Weber HP, Lang NP. Tissue integration of non-submerged implants. 1-year results of a prospective study with 100 ITI hollow-cylinder and hollow-screw implants. Clin Oral Implants Res 1990;1:33-40.
28. Buser D, Weber HP, Bragger U, Balsiger C. Tissue integration of one-stage ITI implants: 3-year results of a longitudinal study with Hollow-Cylinder and Hollow-Screw implants. The International journal of oral & maxillofacial implants 1991;6:405-412.
29. Buser D, Mericske-Stern R, Bernard JP, Behneke A, Behneke N, Hirt HP, et al. Long-term evaluation of non-submerged ITI implants. Part 1: 8-year life table analysis of a prospective multi-center study with 2359 implants. Clin Oral Implants Res 1997;8:161-172.
30. Roccuzzo M, Bunino M, Prioglio F, Bianchi SD. Early loading of sandblasted and acid-etched (SLA) implants: a prospective split-mouth comparative study. Clin Oral Implants Res 2001;12:572-578.
31. Lazarof S, Sumiya Hobo, and Hessam Nowzari. The immediate load implant system: esthetic implant dentistry for the 21st century. Chicago: Quintessence, 1998.
32. Jiménez-López V, Thomas P. Keogh, and Thomas P. Keogh. Immediate loading in implant dentistry: surgical, prosthetic, occlusal, and laboratory aspects. Barcelona: Editorial Quintessence, 2005.
33. Raghavendra S, Wood MC, Taylor TD. Early wound healing around endosseous implants: a review of the literature. The International journal of oral & maxillofacial implants 2005;20:425-431.
34. Ahn S-J. Differences in implant stability associated with various methods of preparation of the implant bed: An in vitro study. The Journal of Prosthetic Dentistry 2012;107:366-372.

35. Berglundh T, Abrahamsson I, Lang NP, Lindhe J. De novo alveolar bone formation adjacent to endosseous implants. Clin Oral Implants Res 2003;14:251-262.
36. Lorenzoni M, Pertl C, Zhang K, Wimmer G, Wegscheider WA. Immediate loading of single-tooth implants in the anterior maxilla. Preliminary results after one year. Clin Oral Implants Res 2003;14:180-187.
37. Testori T, Del Fabbro M, Szmukler-Moncler S, Francetti L, Weinstein RL. Immediate occlusal loading of Osseotite implants in the completely edentulous mandible. The International journal of oral & maxillofacial implants 2003;18:544-551.
38. Ottoni JM, Oliveira ZF, Mansini R, Cabral AM. Correlation between placement torque and survival of single-tooth implants. The International journal of oral & maxillofacial implants 2005;20:769-776.
39. Teerlinck J, Quirynen M, Darius P, van Steenberghe D. Periotest: an objective clinical diagnosis of bone apposition toward implants. The International journal of oral & maxillofacial implants 1991;6:55-61.
40. Meredith N, Alleyne D, Cawley P. Quantitative determination of the stability of the implant-tissue interface using resonance frequency analysis. Clin Oral Implants Res 1996;7:261-267.
41. Meredith N, Shagaldi F, Alleyne D, Sennerby L, Cawley P. The application of resonance frequency measurements to study the stability of titanium implants during healing in the rabbit tibia. Clin Oral Implants Res 1997;8:234-243.
42. Friberg B, Sennerby L, Linden B, Grondahl K, Lekholm U. Stability measurements of one-stage Branemark implants during healing in mandibles. A clinical resonance frequency analysis study. Int J Oral Maxillofac Surg 1999;28:266-272.
43. Cornelini R, Cangini F, Covani U, Barone A, Buser D. Immediate restoration of single-tooth implants in mandibular molar sites: a 12-month preliminary report. The International journal of oral & maxillofacial implants 2004;19:855-860.
44. The Implant Stability Quotient Whitebook. 2010.
45. Nedir R, Bischof M, Szmukler-Moncler S, Bernard JP, Samson J. Predicting osseointegration by means of implant primary stability. Clin Oral Implants Res 2004;15:520-528.
46. Convissar RA. Principles and practice of laser dentistry. St. Louis, Mo.: Mosby Elsevier, 2011.
47. Hamblin MR DT. Mechanisms of Low Level Light Therapy. Proc SPIE 2006;Vol 6140.
48. Barolet D. Light-Emitting Diodes (LEDs) in Dermatology. Semin Cutan Med Surg 2008;27:227-238.
49. Nobel Lectures, Physiology or Medicine 1901-1921. Amsterdam: Elsevier Publishing Company, 1967.
50. Roelandts R. A new light on Niels Finsen, a century after his Nobel Prize. Photodermatol Photoimmunol Photomed 2005;21:115-117.
51. Maiman TH. Stimulated optical radiation in ruby. Nature 1969;187:493–494.
52. Kishen A, & Asundi, A. . fundamentals and application of biophotonics in dentistry. London: Imperial College Press, 2007.

53. Mester E, Szende B, Gartner P. [The effect of laser beams on the growth of hair in mice]. Radiobiol Radiother 1968;9:621-626.
54. Huang YY, Sharma SK, Carroll J, Hamblin MR. Biphasic dose response in low level light therapy - an update. Dose Response 2011;9:602-618.
55. Chung H, Dai T, Sharma SK, Huang YY, Carroll JD, Hamblin MR. The nuts and bolts of low-level laser (light) therapy. Ann Biomed Eng 2012;40:516-533.
56. The American Heritage dictionary of the English language. Boston: Houghton Mifflin, 1992.
57. Einstein A. zur quantum theorie der stralung. Phys Z 1917:121-128.
58. Karu T. Photobiology of low-power laser effects. Health Phys 1989;56:691-704.
59. Kasap S. pn junction devices and light emitting diodes. University of Saskatchewan, Canada, 2001.
60. Kasap SO. Principles of Electronic Materials and Devices. New York: McGraw-Hill, 2006.
61. Whelan HT, Buchmann EV, Dhokalia A, Kane MP, Whelan NT, Wong-Riley MT, et al. Effect of NASA light-emitting diode irradiation on molecular changes for wound healing in diabetic mice. J Clin Laser Med Surg 2003;21:67-74.
62. Whelan HT, Smits RL, Jr., Buchman EV, Whelan NT, Turner SG, Margolis DA, et al. Effect of NASA light-emitting diode irradiation on wound healing. J Clin Laser Med Surg 2001;19:305-314.
63. Moritz A, & Beer, F. Oral laser application. London: Quintessence, 2006.
64. Ojeda A RE. Analysis of light-emission processes in light-emitting diodes and semiconductor lasers. Eur J Phys 1997;18:63–67.
65. Karu T. Laser biostimulation: a photobiological phenomenon. J Photochem Photobiol B 1989;3:638-640.
66. Peplow PV, Chung TY, Baxter GD. Laser photobiomodulation of wound healing: a review of experimental studies in mouse and rat animal models. Photomedicine and laser surgery 2010;28:291-325.
67. Desmet KD, Paz DA, Corry JJ, Eells JT, Wong-Riley MT, Henry MM, et al. Clinical and experimental applications of NIR-LED photobiomodulation. Photomedicine and laser surgery 2006;24:121-128.
68. Patrice T. Photodynamic Therapy. UK: Royal Society of Chemistry, 2003.
69. Guyton AC, Hall JE. Textbook of medical physiology. Philadelphia: Elsevier Saunders, 2006.
70. Alberts B. Molecular Biology of the Cell. New York: Garland Science, 2008.
71. Karp G. Cell and Molecular Biology: Concepts and Experiments: Wiley, 2009.
72. Davey J, Lord M. Essential cell biology : a practical approach. Oxford ; New York: Oxford University Press, 2003.
73. Vander AJ, Sherman JH, Luciano DS. Human physiology : the mechanisms of body function. Boston, Mass.: WCB McGraw-Hill, 2001.
74. Mitchell P. Coupling of phosphorylation to electron and hydrogen transfer by a chemi-osmotic type of mechanism. Nature 1961;191:144-148.
75. Karu TI, Kolyakov SF. Exact action spectra for cellular responses relevant to phototherapy. Photomedicine and laser surgery 2005;23:355-361.

76. Yu W, Naim JO, McGowan M, Ippolito K, Lanzafame RJ. Photomodulation of oxidative metabolism and electron chain enzymes in rat liver mitochondria. Photochem Photobiol 1997;66:866-871.
77. Turrens JF. Mitochondrial formation of reactive oxygen species. J Physiol 2003;552:335-344.
78. Karu TI, Pyatibrat LV, Afanasyeva NI. Cellular effects of low power laser therapy can be mediated by nitric oxide. Lasers in surgery and medicine 2005;36:307-314.
79. Hamblin M. The role of nitric oxide in low level light therapy. Proc SPIE 2008;6846.
80. Moriyama Y, Moriyama EH, Blackmore K, Akens MK, Lilge L. In vivo study of the inflammatory modulating effects of low-level laser therapy on iNOS expression using bioluminescence imaging. Photochem Photobiol 2005;81:1351-1355.
81. Karu T. Primary and secondary mechanisms of action of visible to near-IR radiation on cells. J Photochem Photobiol B 1999;49:1-17.
82. Stief TW. The physiology and pharmacology of singlet oxygen. Med Hypotheses 2003;60:567-572.
83. Thannickal VJ, Fanburg BL. Reactive oxygen species in cell signaling. Am J Physiol Lung Cell Mol Physiol 2000;279:L1005-1028.
84. Gonzalez-Rubio M, Voit S, Rodriguez-Puyol D, Weber M, Marx M. Oxidative stress induces tyrosine phosphorylation of PDGF alpha-and beta-receptors and pp60c-src in mesangial cells. Kidney Int 1996;50:164-173.
85. Roveri A, Coassin M, Maiorino M, Zamburlini A, van Amsterdam FT, Ratti E, et al. Effect of hydrogen peroxide on calcium homeostasis in smooth muscle cells. Arch Biochem Biophys 1992;297:265-270.
86. Grover AK, Samson SE, Fomin VP. Peroxide inactivates calcium pumps in pig coronary artery. Am J Physiol 1992;263:H537-543.
87. Neumann JT, Diaz-Sylvester PL, Fleischer S, Copello JA. CGP-37157 inhibits the sarcoplasmic reticulum Ca(2)+ ATPase and activates ryanodine receptor channels in striated muscle. Mol Pharmacol 2011;79:141-147.
88. Meyer M, Schreck R, Baeuerle PA. H2O2 and antioxidants have opposite effects on activation of NF-kappa B and AP-1 in intact cells: AP-1 as secondary antioxidant-responsive factor. Embo J 1993;12:2005-2015.
89. Schreck R, Albermann K, Baeuerle PA. Nuclear factor kappa B: an oxidative stress-responsive transcription factor of eukaryotic cells (a review). Free Radic Res Commun 1992;17:221-237.
90. Hayden MS, Ghosh S. Signaling to NF-kappaB. Genes Dev 2004;18:2195-2224.
91. Gilmore T. The Rel/NF-kappaB Signal Transduction Pathway. NF-kB Transcription Factors. Biology Department, Boston University.
92. Gilmore TD. Introduction to NF-kappaB: players, pathways, perspectives. Oncogene 2006;25:6680-6684.
93. Schafer FQ, Buettner GR. Redox environment of the cell as viewed through the redox state of the glutathione disulfide/glutathione couple. Free Radic Biol Med 2001;30:1191-1212.
94. Liu H, Colavitti R, Rovira, II, Finkel T. Redox-dependent transcriptional regulation. Circ Res 2005;97:967-974.

95. Hirota K, Murata M, Sachi Y, Nakamura H, Takeuchi J, Mori K, et al. Distinct roles of thioredoxin in the cytoplasm and in the nucleus. A two-step mechanism of redox regulation of transcription factor NF-kappaB. J Biol Chem 1999;274:27891-27897.
96. Rainwater R, Parks D, Anderson ME, Tegtmeyer P, Mann K. Role of cysteine residues in regulation of p53 function. Mol Cell Biol 1995;15:3892-3903.
97. Barrett WC, DeGnore JP, Keng YF, Zhang ZY, Yim MB, Chock PB. Roles of superoxide radical anion in signal transduction mediated by reversible regulation of protein-tyrosine phosphatase 1B. J Biol Chem 1999;274:34543-34546.
98. Karu TI, Pyatibrat LV, Kolyakov SF, Afanasyeva NI. Absorption measurements of a cell monolayer relevant to phototherapy: reduction of cytochrome c oxidase under near IR radiation. J Photochem Photobiol B 2005;81:98-106.
99. Dall Agnol MA, Nicolau RA, de Lima CJ, Munin E. Comparative analysis of coherent light action (laser) versus non-coherent light (light-emitting diode) for tissue repair in diabetic rats. Lasers in medical science 2009;24:909-916.
100. Ying R, Liang HL, Whelan HT, Eells JT, Wong-Riley MT. Pretreatment with near-infrared light via light-emitting diode provides added benefit against rotenone- and MPP+-induced neurotoxicity. Brain Res 2008;3:167-173.
101. Yazdani SO, Golestaneh AF, Shafiee A, Hafizi M, Omrani HA, Soleimani M. Effects of low level laser therapy on proliferation and neurotrophic factor gene expression of human schwann cells in vitro. J Photochem Photobiol B 2012;107:9-13.
102. Medalha CC, Di Gangi GC, Barbosa CB, Fernandes M, Aguiar O, Faloppa F, et al. Low-level laser therapy improves repair following complete resection of the sciatic nerve in rats. Lasers in medical science 2012;27:629-635.
103. Rochkind S. Phototherapy in peripheral nerve regeneration: From basic science to clinical study. Neurosurg Focus 2009;26.
104. Gigo-Benato D, Geuna S, Rochkind S. Phototherapy for enhancing peripheral nerve repair: a review of the literature. Muscle Nerve 2005;31:694-701.
105. Shen CC, Yang YC, Liu BS. Effects of large-area irradiated laser phototherapy on peripheral nerve regeneration across a large gap in a biomaterial conduit. J Biomed Mater Res A 2012;10:34314.
106. Miloro M, Halkias LE, Mallery S, Travers S, Rashid RG. Low-level laser effect on neural regeneration in Gore-Tex tubes. Oral surgery, oral medicine, oral pathology, oral radiology, and endodontics 2002;93:27-34.
107. Anders JJ, Borke RC, Woolery SK, Van de Merwe WP. Low power laser irradiation alters the rate of regeneration of the rat facial nerve. Lasers in surgery and medicine 1993;13:72-82.
108. Khullar SM, Brodin P, Barkvoll P, Haanaes HR. Preliminary study of low-level laser for treatment of long-standing sensory aberrations in the inferior alveolar nerve. J Oral Maxillofac Surg 1996;54:2-7.
109. Khullar SM, Emami B, Westermark A, Haanaes HR. Effect of low-level laser treatment on neurosensory deficits subsequent to sagittal split ramus osteotomy. Oral surgery, oral medicine, oral pathology, oral radiology, and endodontics 1996;82:132-138.

110. Miloro M, Repasky M. Low-level laser effect on neurosensory recovery after sagittal ramus osteotomy. Oral surgery, oral medicine, oral pathology, oral radiology, and endodontics 2000;89:12-18.
111. Agha-Hosseini F, Moslemi E, Mirzaii-Dizgah I. Comparative evaluation of low-level laser and CO(2) laser in treatment of patients with oral lichen planus. Int J Oral Maxillofac Surg 2012;9:9.
112. Artés-Ribas M, Arnabat-Dominguez J, Puigdollers A. Analgesic effect of a low-level laser therapy (830 nm) in early orthodontic treatment. Lasers in medical science:1-7.
113. Bicakci AA, Kocoglu-Altan B, Toker H, Mutaf I, Sumer Z. Efficiency of low-level laser therapy in reducing pain induced by orthodontic forces. Photomedicine and laser surgery 2012;30:460-465.
114. Ferrante M, Petrini M, Trentini P, Perfetti G, Spoto G. Effect of low-level laser therapy after extraction of impacted lower third molars. Lasers in medical science 2012;28:28.
115. Simoes A, Eduardo FP, Luiz AC, Campos L, Sa PH, Cristofaro M, et al. Laser phototherapy as topical prophylaxis against head and neck cancer radiotherapy-induced oral mucositis: comparison between low and high/low power lasers. Lasers in surgery and medicine 2009;41:264-270.
116. Kulekcioglu S, Sivrioglu K, Ozcan O, Parlak M. Effectiveness of low-level laser therapy in temporomandibular disorder. Scand J Rheumatol 2003;32:114-118.
117. Jang H, Lee H. Meta-analysis of pain relief effects by laser irradiation on joint areas. Photomedicine and laser surgery 2012;30:405-417.
118. Pinheiro AL, Gerbi ME. Photoengineering of bone repair processes. Photomedicine and laser surgery 2006;24:169-178.
119. Khadra M, Lyngstadaas SP, Haanaes HR, Mustafa K. Effect of laser therapy on attachment, proliferation and differentiation of human osteoblast-like cells cultured on titanium implant material. Biomaterials 2005;26:3503-3509.
120. Ueda Y, Shimizu N. Effects of pulse frequency of low-level laser therapy (LLLT) on bone nodule formation in rat calvarial cells. J Clin Laser Med Surg 2003;21:271-277.
121. Kim YD, Song WW, Kim SS, Kim GC, Hwang DS, Shin SH, et al. Expression of receptor activator of nuclear factor -kappaB ligand, receptor activator of nuclear factor -kappaB, and osteoprotegerin, following low-level laser treatment on deproteinized bovine bone graft in rats. Lasers in medical science 2009;24:577-584.
122. Kim YD, Kim SS, Kim SJ, Kwon DW, Jeon ES, Son WS. Low-level laser irradiation facilitates fibronectin and collagen type I turnover during tooth movement in rats. Lasers in medical science 2010;25:25-31.
123. Pyo SJ, Song WW, Kim IR, Park BS, Kim CH, Shin SH, et al. Low-level laser therapy induces the expressions of BMP-2, osteocalcin, and TGF-beta1 in hypoxic-cultured human osteoblasts. Lasers in medical science 2012;3:3.
124. Khadra M, Kasem N, Haanaes HR, Ellingsen JE, Lyngstadaas SP. Enhancement of bone formation in rat calvarial bone defects using low-level laser therapy. Oral surgery, oral medicine, oral pathology, oral radiology, and endodontics 2004;97:693-700.

125. Khadra M, Ronold HJ, Lyngstadaas SP, Ellingsen JE, Haanaes HR. Low-level laser therapy stimulates bone-implant interaction: an experimental study in rabbits. Clin Oral Implants Res 2004;15:325-332.
126. Khadra M, Kasem N, Lyngstadaas SP, Haanaes HR, Mustafa K. Laser therapy accelerates initial attachment and subsequent behaviour of human oral fibroblasts cultured on titanium implant material. A scanning electron microscope and histomorphometric analysis. Clin Oral Implants Res 2005;16:168-175.
127. Khadra M, Lyngstadaas SP, Haanaes HR, Mustafa K. Determining optimal dose of laser therapy for attachment and proliferation of human oral fibroblasts cultured on titanium implant material. J Biomed Mater Res A 2005;73:55-62.
128. Pinheiro AL, Martinez Gerbi ME, de Assis Limeira F, Jr., Carneiro Ponzi EA, Marques AM, Carvalho CM, et al. Bone repair following bone grafting hydroxyapatite guided bone regeneration and infra-red laser photobiomodulation: a histological study in a rodent model. Lasers in medical science 2009;24:234-240.
129. Ball KA, Castello PR, Poyton RO. Low intensity light stimulates nitrite-dependent nitric oxide synthesis but not oxygen consumption by cytochrome c oxidase: Implications for phototherapy. J Photochem Photobiol B 2011;102:182-191.
130. Raosoft I. 2004.
131. Cawood JI, Howell RA. A classification of the edentulous jaws. Int J Oral Maxillofac Surg 1988;17:232-236.
132. Dental Implant Systems. 2012.
133. Bischof M, Nedir R, Szmukler-Moncler S, Bernard JP, Samson J. Implant stability measurement of delayed and immediately loaded implants during healing. Clin Oral Implants Res 2004;15:529-539.
134. Ivanoff CJ, Sennerby L, Johansson C, Rangert B, Lekholm U. Influence of implant diameters on the integration of screw implants. An experimental study in rabbits. Int J Oral Maxillofac Surg 1997;26:141-148.
135. Ivanoff CJ, Grondahl K, Sennerby L, Bergstrom C, Lekholm U. Influence of variations in implant diameters: a 3- to 5-year retrospective clinical report. The International journal of oral & maxillofacial implants 1999;14:173-180.
136. Kessler-Liechti G, Zix J, Mericske-Stern R. Stability measurements of 1-stage implants in the edentulous mandible by means of resonance frequency analysis. The International journal of oral & maxillofacial implants 2008;23:353-358.
137. Lazzara RJ, Porter SS. Platform switching: a new concept in implant dentistry for controlling postrestorative crestal bone levels. The International journal of periodontics & restorative dentistry 2006;26:9-17.
138. Cochran DL, Hermann JS, Schenk RK, Higginbottom FL, Buser D. Biologic width around titanium implants. A histometric analysis of the implanto-gingival junction around unloaded and loaded nonsubmerged implants in the canine mandible. J Periodontol 1997;68:186-198.
139. Quirynen M, Naert I, van Steenberghe D. Fixture design and overload influence marginal bone loss and fixture success in the Branemark system. Clin Oral Implants Res 1992;3:104-111.
140. Hermann JS, Cochran DL, Nummikoski PV, Buser D. Crestal bone changes around titanium implants. A radiographic evaluation of unloaded nonsubmerged

and submerged implants in the canine mandible. J Periodontol 1997;68:1117-1130.
141. Hermann JS, Buser D, Schenk RK, Cochran DL. Crestal bone changes around titanium implants. A histometric evaluation of unloaded non-submerged and submerged implants in the canine mandible. J Periodontol 2000;71:1412-1424.
142. Hermann JS, Schoolfield JD, Nummikoski PV, Buser D, Schenk RK, Cochran DL. Crestal bone changes around titanium implants: a methodologic study comparing linear radiographic with histometric measurements. The International journal of oral & maxillofacial implants 2001;16:475-485.
143. Hermann JS, Jones AA, Bakaeen LG, Buser D, Schoolfield JD, Cochran DL. Influence of a machined collar on crestal bone changes around titanium implants: a histometric study in the canine mandible. J Periodontol 2011;82:1329-1338.